



FACULTY OF SCIENCE AND TECHNOLOGY

BACHELOR THESIS

Study programme / specialisation:

The spring semester, 2022

Bachelor of Science in Petroleum
Technology

Open

Author:

Ine Skartveit Bergsvik

Ine Skartveit Bergsvik
(signature author)

Course coordinator:

Arild Saasen

Supervisor(s):

Arild Saasen

Karl Ronny Klungtvedt

Thesis title:

Optimizing formulations for reservoir drilling fluids

Credits (ECTS): 20

Keywords:

Drilling fluid, CaCO₃, fibers, fluid loss,
formation damage, starch, LMC pills.

Pages: 46

+ appendix: 6

Stavanger, 29th May/2022
date/year

Acknowledgement

I would like to thank European Mud Company (EMC) for providing a professional laboratory environment set up to collect high quality test data. The people at EMC provided a valuable learning experience. Karl Ronny Klungvedt was a great supervisor, providing valuable knowledge and advice related to analysis and visualization of test results. It has been a pleasure cooperating with Bjørn Berglind in the laboratory, who has generously shared his knowledge and experience from a long career in the field. Jan Kristian Vasshus was helpful in facilitating good test conditions in the lab.

I would also like to thank my supervisor from University of Stavanger, Arild Saasen, for excellent follow-up and feedback throughout the process.

Abstract

When drilling a well, equivalent circulation density exceeding the fracture gradient can cause lost circulation. In a reservoir section, invasion of drilling fluids can potentially cause a permanent permeability reduction in the near wellbore area, which can be detrimental to well productivity. Low-permeable filter cakes that reduce fluid loss and are easily removed during drawdown are desirable to prevent damaging the formation.

The main focus of the thesis is to find formulations for low-permeable formation drilling fluids that prevents loss to the formation and simultaneously prevent formation damage. Fluid properties for fractured scenarios in a reservoir zone are also investigated.

Eleven samples of conventional drilling fluids and five samples of Lost Circulation Material (LCM) pills for severe losses were prepared with varying concentrations and additives. Calcium carbonate (CaCO_3) and fibers were added as LCM, while modified and crosslinked potato starch were used as filtration control polymers. HTHP fluid loss tests of conventional drilling fluids were performed on porous discs and filter paper, while pressure tests of LCM pills were performed on tapered discs.

The results show how addition of fibers in conventional drilling fluids with CaCO_3 as LCM may improve sealing capabilities and maintain low formation damage when containing effective filtration control polymers. For LCM pills, addition of CaCO_3 may regulate the thickness of the filter cake and the ability to remove it.

Nomenclature

AHR – After Hot-Rolling

BHA- Bottom Hole Assembly

BHR – Before Hot-Rolling

BRIX – Refraction degree (sugar content of an aqueous solution)

CPR – Crosslinked Potato Starch

HHP – High Temperature High Pressure

LCM – Lost Circulation Material

NIF – Non-Invasive Fluid

OD – Outer Diameter

PHP – Peak Hold Pressure

PSD – Particle Size Distribution

SHP – Sustainable Hold Pressure

List of Contents

Acknowledgement	2
Abstract	3
Nomenclature.....	4
List of Contents.....	5
List of Figures	7
List of Tables.....	9
1. Introduction	10
2. Theory	14
2.1. <i>Fluid mixing</i>	14
2.2. <i>Particle Size Distribution (PSD)</i>	16
2.3. <i>Rheology</i>	17
2.4. <i>Formation damage</i>	18
2.4.1. Fluid loss; ceramic disc and filter paper.....	18
2.4.2. Reverse flow and filter cake removal.....	19
2.4.3. Disc mass.....	20
2.4.4. Permeability	21
2.4.5. Fluid filtrate analysis	22
2.5. <i>Pressure logging on tapered disc with differential pressure > 1000 psi (6.9 MPa)</i> 22	
3. Experimental work, results and discussion.....	24
3.1. <i>Degradation of PSD</i>	25
3.1.1. Effect of mechanical degradation on CaCO ₃	25
3.1.2. Effect of mechanical degradation on fiber	26
3.1.3. Effect on fluid loss	27
3.2. <i>Different PSD compositions of CaCO₃ and the effect of adding fiber</i>	28

3.2.1. Viscosity parameters	28
3.2.2. Fluid loss	30
3.2.3. Disc mass and permeability.....	32
3.2.4. Fluid filtrate.....	34
3.3. <i>Effect of changing starch type</i>	36
3.3.1. Viscosity parameters	36
3.3.2. Fluid loss	38
3.3.3. Disc mass and permeability.....	39
3.4. <i>Effect of using CaCO₃ in LCM pills</i>	41
3.4.1. Differential sealing pressure.....	41
3.4.2. Lift off pressure	43
4. Sources of error / Lessons learned.....	44
5. Conclusion.....	45
6. References	46
Appendix A	47
Appendix B.....	49
Appendix C	51
Appendix D	52

List of Figures

Figure 2-1: Hamilton Beach Mixer to the left, Ohaus Pioneer Precision PX3202 in the middle, Ofite roller-oven #172-00-1-C to the right.....	15
Figure 2-2: Equipment for wet-sieving fluids, to measure particle size distribution.....	16
Figure 2-3: Ofite Viscometer model 900.	17
Figure 2-4: Ofite Filter Press HTHP 175 mL Double Capped to the left, fluid cell to the upper right, DVP EC.20-1 vacuum machine to the lower right.	18
Figure 2-5: Ceramic disc used for fluid loss tests.	19
Figure 2-6: Transparent cylinder, Festo Pressure regulator LRP-1/4-2.5 and LRP-1/4-0.25, Festo Pressure Sensor SPAN-P025R and SPAN-P10R, Fest Flowmeter SFAH-10U.....	19
Figure 2-7: Ohaus MB120 Moisture Analyzer.	20
Figure 2-8: Festo Pressure regulator LRP-1/4-2.5 and LRP-1/4-0.25, Festo Pressure Sensor SPAN-PO25R and SPAN-P10R, Festo Flowmeter SFAH-10U, cell for disc insert.	21
Figure 2-9: Hanna Instruments Sucrose Refractometer HI 96801 to the left, Eutech Expert CTS to the right.....	22
Figure 2-10: Permeability Plugging Apparatus to the left, main parts of the insert in the middle, pressure and logging device to the right.	23
Figure 2-11: Tapered discs used for pressure testing and filter cake removal.....	23
Figure 3-1: PSD of Sample 1, a fluid with CaCO ₃ up to 53 μm before (BHR) and after hot-rolling using grinding rod (AHR-ROD).....	25
Figure 3-2: PSD of Sample 2, a fluid with CaCO ₃ up to 23 μm and fiber (Additive 1) before (BHR) and after hot-rolling using grinding rod (AHR-ROD).	26
Figure 3-3: Fluid loss curves for fluid with only CaCO ₃ (Base – no rod) and fluid with a combination of CaCO ₃ and fiber both with grinding rod (Base + Additive 2 – with rod) and without grinding rod (Base + Additive 1 – no rod) on 120 μm discs with 1000 psi (6.9 MPa) differential pressure.....	27
Figure 3-4: Viscosity measurements with shear rates in range 0-1000 (1/s) in 1) and 0-300 (1/s) in 2) of fluids with only CaCO ₃ in a) and fluid with addition of fiber in b).....	29
Figure 3-5: Fluid loss on 10, 20 and 120 μm discs for 30 minutes. Fluids with only CaCO ₃ in a) and fluids with addition of fiber in b).	30
Figure 3-6: Disc mass increase and retained permeability of 10, 20, and 120 μm discs. Fluids with only CaCO ₃ in a) and fluids with addition of fiber in b).....	32

Figure 3-7: Amount polymers in the fluid filtrate from 11 and 20-25 μm filter paper tests (500 psi) in 1) and 10 and 20 μm disc tests (1000 and 750 psi) in 2). Fluids with only CaCO_3 in a) and fluids with addition of fiber in b).	34
Figure 3-8: Viscosity measurements with shear rates in range 0-1000 (1/s) in 1) and 0-300 (1/s) in 2) of fluids with crosslinked potato starch in a) and fluids with modified starch in b).	37
Figure 3-9: Fluid loss in 30 minutes for fluids with crosslinked potato starch and fluids with modified starch on 10 μm discs.	38
Figure 3-10: Disc mass increase and retained permeability for fluids with crosslinked potato starch and fluids with modified starch on 10 μm discs.	39
Figure 3-11: Maximum measured sealing pressure on tapered discs with different fracture sizes for LCM pills containing only CaCO_3 (Pill 1), only fiber (Pill 3 and 5) and both CaCO_3 and fiber (Pill 2 and 4). White indicators represent CaCO_3 in the formulation.	41
Figure 3-12: Pressure needed to remove the filter cake enough for brine to flow through the fracture for LCM pills containing only CaCO_3 (Pill 1), only fiber (Pill 3 and 5) and both CaCO_3 and fiber (Pill 2 and 4). White indicator represents addition of CaCO_3	43
Figure C-1: Tapered discs after pressure tests for pills with inclusion of CaCO_3	51
Figure C-2: Tapered discs after pressure tests for pills with no CaCO_3	51
Figure D-1: Discs with filter cakes for fluids with crosslinked potato starch and fluids with modified starch after fluid loss tests.	52
Figure D-2: Discs used for testing fluids with crosslinked potato starch and fluids with modified starch, after filter cake removal with reverse flow.	52

List of Tables

Table 2-1: Components used in this thesis.....	14
Table 3-1: Overview of fluids used for samples in the thesis.....	24
Table B-1: Recipe and mixing sequence for samples 1-8 in grams unless stated otherwise ...	49
Table B-2: Recipe and mixing sequence for fluid with crosslinked potato starch (Samples 9-11) in grams unless stated otherwise.....	49
Table B-3: Name and amount additives used in the mixtures.....	50
Table B-4: Recipe for LCM Pills (Samples 12-16) in grams unless stated otherwise.....	50

1. Introduction

When drilling a well, at least two barriers are always necessary, and the primary barrier during drilling is drilling fluid. A drilling fluid has several purposes, and a key purpose is to maintain borehole stability. To keep the well stable, it is necessary to maintain a certain equivalent circulation density (ECD), which is the pressure drop in the annulus combined with hydrostatic weight. If the ECD is below the pore-pressure gradient, there is a risk of influx from the formation into the well. Vice versa, if the ECD exceeds the fracture gradient, lost circulation may occur. This explains why it is necessary that the ECD is kept between the pore-pressure gradient and the fracture gradient during drilling.

Selection of drilling fluids depend, among other things, on the lithology and temperature of the formation, well trajectory and pressure. As the fluid flows through the drill bit nozzles, one of the functions of a drilling fluid is to cool and lubricate the bit. A consequence of circulating through the bit, is that the drilling fluid is exposed to mechanical wear. In addition, the temperature of the well contributes to thermal wear. When testing drilling fluids, it is important that the testing represents the field conditions. Therefore, to account for the wear due to circulation, hot-rolling of the drilling fluid at a representative temperature is part of normal testing procedure. Klungtvedt and Saasen (2022a) tested an extended method to simulate mechanical wear during circulation by placing a threaded steel rod into the hot-rolling cell with preventative LCM fluid samples with different additives. Lost circulation tests were done for similar fluids prepared with and without the steel rod. By comparing the results of the respective fluids, they found that the sealing performance of the materials was strongly differentiated. In this thesis, the same method for hot-rolling was used to conduct fluid loss test for drilling fluids designed for permeable formations. This was done to better understand how the impact of mechanical degradation affects the particle size distribution (PSD) of different materials, and thus, the fluid loss to the formation.

The drill bit will cause pieces of rock with different sizes, commonly known as cuttings, to detach from the formation. A function of the drilling fluid is to lift the cuttings out of the annulus. The ejecting effect of the fluid due to the nozzle diameter being much smaller than the diameter of the drill string, cleans the area around the bit. To obtain proper hole cleaning, rheological properties are important. A shear-thinning fluid has decreased viscosity with increased shear stress. This means that when flowing through the drill bit where the shear stress

is high, the viscosity is low. When flowing in the annulus where the shear stress is lower, the viscosity is higher. A certain gel strength is also necessary to prevent sag of the cuttings when there is no circulation.

Different factors must be considered when designing a drilling fluid, and additives are used to ensure the properties of the fluid are achieved. For a water-based reservoir fluid, polymers such as xanthan gum and starch are added to reduce fluid loss and provide viscosity. Khan et al. (2007) showed that such polymers might help to reduce fluid loss. However, when pore-throats and differential pressures exceeds 20 μm and 500 psi (3.45 MPa) respectively, addition of such polymers may have little effect on preventing solids to enter the formation. An experimental analysis to measure the relative polymer concentration in the filtrate was conducted by Klungtvedt and Saasen (2022d). They found that when cellulose-based particles were present in the filter cake, the polymer invasion to the formation was reduced relative to a fluid with calcium carbonate (CaCO_3) as the only bridging material. Solids are added to help achieve the properties of the fluid. As one of the functions of a drilling fluid is to maintain a stable well, by keeping ECD between the fracture gradient and pore-pressure gradient, weighting material is used to regulate the density. Barite is a common weighting material in both oil- and water-based drilling fluids due to its high density. Dissolved sodium chloride (NaCl) and CaCO_3 does also function as weighting agents, but with lower density. CaCO_3 is cheap and acid-soluble material with a density of 2.7 s.g. It is also used as a bridging material to create a low permeable filter cake and reduce fluid invasion to the formation.

A study performed by Alsaba et al. (2014) showed that for sealing wide fractures with drilling fluids with conventional LCM, fibrous material resulted in the best sealing performance and ability to maintain the integrity of the seal on tapered discs. They concluded that it was due to the fibers' wide particle size distribution and irregular shape. Khalifeh et al. (2019) found that the seals could withstand the pressure as it was gradually increased, when testing with fiber-based LCM. Klungtvedt, Saasen, et al. (2021) conducted fluid loss and permeability measurements on permeable discs to investigate the sealing effect of cellulose-based additives. They found that for fluids without solid present as weighting material or drill solid, addition of fiber resulted in reduced fluid loss and formation damage on 20 μm discs. In 2022, Klungtvedt and Saasen (2022b) found that addition of fiber to a KCl-polymer based drilling fluid with CaCO_3 present, may reduce the permeability of the external filter cake.

When a fluid is circulating, it is supposed to form a filter cake on the borehole wall. The thickness of the filter cake can affect the friction applied on the bottom hole assembly (BHA), and a filter cake that is too thick can potentially result in differential pressure sticking. To prevent this, it is desirable that the drilling fluid creates a thin filter cake (Skjeggstad, 1989). A drilling fluid should in addition have specific properties when drilling in reservoir sections, because drilling fluids has the potential to damage formation and reduce production from the reservoir. Low fluid loss is desirable to prevent damaging the near wellbore zone, hence the drilling fluid should form a low-permeable filter cake that can be easily removed during drawdown. A study by Green et al. (2017) showed that the lowest fluid loss did not directly correspond with the lowest change in permeability. They concluded it was more likely that the major formation damage was caused by the ability of the filter cake to stick to the formation and whether it is removable during production. Different particle sizes can be used to regulate the ability to form a removable external filter cake rather than a permanent internal filter cake.

If drilling fluid penetrates a producing formation, the permeability in the near wellbore area might decrease, resulting in an additional pressure drop and poor production efficiency. This damage can sometimes be repaired, and a test series on permeable disc conducted by Klungtvedt, Khalifeh, et al. (2021) showed that an oxidation breaker effectively removed the filter cake when applied with a typical reservoir temperature. Weight measurements and visual inspection indicated that even before applying reverse pressure, application of breaker may result in a large amount of the original permeability being restored. Application of breaker will not be reported in this thesis. Reduced permeability in the near wellbore may also be permanent, which can be detrimental to well productivity. Hence a drilling fluid preventing formation damage with high retained permeability is desirable.

Evaluation of formation damage is typically done with core flooding tests of representative samples from formations near the wellbore. The use of such samples can be inefficient, expensive, and inaccessible. Klungtvedt and Saasen (2022c) has developed a time and cost-effective method for assessing formation damage on permeable ceramic discs. The discs are weighed during different stages of testing, and the permeability to air and water are measured before fluid invasion and after reversed pressure and fluid flow, resulting in a value for mass increase and retained permeability.

During drilling operations, encountering high permeability fractures can result in severe fluid loss and well control problems. In a reservoir section, fracture permeability can be important for production, especially in low permeability reservoirs. Hence, it is important to minimize permanent fluid damage in fractures. The primary focus of this thesis is to investigate how additives impact the properties of drilling fluids in low permeable reservoirs, but some tests also address fractured scenarios.

The objectives of the study were to investigate:

- How particle degradation of CaCO_3 and fiber material due to mechanical wear impacts the sealing ability when used as LCM in a drilling fluid.
- How fluids with different particle size CaCO_3 as LCM impacts fluid loss, formation damage and polymer concentration in the filtrate.
- How a combination of CaCO_3 and fiber as LCM impacts fluid loss, formation damage and polymer concentration in the filtrate.
- The effect of changing from modified to crosslinked potato starch on fluid loss and formation damage.
- Whether addition of CaCO_3 can regulate the ability to remove the filter cake from a fracture by using an experimental method for testing reverse pressure.

2. Theory

2.1. Fluid mixing

The test performed in this thesis required preparation of eight drilling fluids and five LCM pills, all water-based fluids. The components used in the samples are listed in Table 2-1. For sodium chloride, fine salt was used in the drilling fluids and sea salt was used in the pills. CaCO_3 was used in a wide range of particle size. The drilling fluids had particles up to 53 μm , and the pills had particles up to 1200 μm .

In laboratory experiments of drilling fluids, 350 mL is used to represent one oilfield barrel (1 bbl). This is practical during mixing, as 1 g in the lab will be equivalent to 1 lbs/bbl. Hence, the sample size used for fluid mixing in the following experiments is 350 mL. For simplicity the components of the drilling fluid are reported in lbs/bbl in the result and discussion section of this thesis.

Table 2-1: Components used in this thesis.

Component	Description / Function
Hydrogen oxide, H_2O , water	
Sodium carbonate, Na_2CO_3 , soda ash	Controlling alkalinity in fluid.
Sodium hydroxide, NaOH , caustic soda	Controlling alkalinity in fluid.
Xanthan Gum, XC (Barazan)	Increase viscosity.
Starch (Dextride E)	Modified starch for controlling fluid loss.
Polymer (N-Dril HT)	Crosslinked starch. Reduce fluid loss.
Magnesium oxide, MgO	Controlling alkalinity in fluid.
Sodium chloride, NaCl , salt	Weighting agent to increase density.
Calcium carbonate, CaCO_3	Bridging agent. Prevent fluid invasion. Weighting material.
Additive 1 (FEBRICOAT C)	Cellulose based NIF. Seal permeable formations.
Additive 2 (AURACOAT UF)	Cellulose based NIF. Reduce formation damage. Finer particles than Additive 3.
Additive 3 (AURACOAT F)	Cellulose based NIF. Reduce formation damage.
Additive 4 (AURAFIX UF)	Cellulose based NIF. Seepage control.
Additive 5 (AURACOAT C)	Cellulose based NIF. Seal permeable formation.
Additive 6 (AURABRIDGE)	Cellulose based LCM.

The recipes in mixing order for all drilling fluids and pills are attached in Appendix B. The components were weighted on a Ohaus Pioneer Precision weight, before mixed with a Hamilton Beach Mixer. The drilling fluids were put in a cell in a roller-oven, and hot-rolled with a temperature of 112 °C for 16 hours, with the purpose of creating a similar environment as for a fluid in a circulation system in a reservoir zone. All drilling fluid samples for disc and filter paper testing were hot-rolled with a threaded steel rod inside the cell, unless stated otherwise. This was done to create a mechanical degradation effect in addition to the degradation effect from the temperature. The equipment used are shown in Figure 2-1.



Figure 2-1: Hamilton Beach Mixer to the left, Ohaus Pioneer Precision PX3202 in the middle, Ofite roller-oven #172-00-1-C to the right.

2.2. Particle Size Distribution (PSD)

Six sieving pans with sieve sizes 53, 75, 90, 125, 150 and 180 μm were used. Each was weighted on Ohaus Pioneer Precision before stacked in ascending order. BHR, drilling fluids were sieved through the stack with water and air pressure, before each sieve was dried and weighted again. The same procedure was done for the drilling fluids AHR to observe potential changes in PSD. The equipment used for fluid sieving is shown in Figure 2-2.



Figure 2-2: Equipment for wet-sieving fluids, to measure particle size distribution.

2.3. Rheology

Before the fluid was put in the hot-roller oven, the viscosity was measured by the viscometer shown in Figure 2-3. When the fluid was out of the roller-oven, the drilling fluid was spun up in the mixer for 3-5 minutes to get rid of possible sag of particles. Viscosity measurements were then repeated, to ensure that the rheological properties were stable. The viscosity was measured at 49 °C for the values of speed in RPM; 1, 2, 3, 6, 10, 20, 30, 60, 100, 200, 300, 600.



Figure 2-3: Ofite Viscometer model 900.

2.4. Formation damage

The permeability measurements were based on the procedure for fluid loss, disc mass and permeability measurements presented in Appendix A, with some modifications.

2.4.1. Fluid loss; ceramic disc and filter paper

A high temperature high pressure (HTHP) filter press was used to perform the fluid loss tests. Ceramic discs with pore throat openings of 10, 20 and 120 μm were soaked in fresh water in a glass beaker before they were put in the vacuum machine to remove any air. The disc was inserted into the filter press cell and drilling mud was added, before the cell was heated to 90 $^{\circ}\text{C}$. A nitrogen source was used to apply a differential pressure of 750 psi (5.2 MPa) on 20 μm disc and 1000 psi (6.9 MPa) on 10 and 120 μm discs. The filtrate was collected in an Erlenmeyer flask placed on a weight. The Ohaus weight logged the amount of fluid in grams on a computer for 30 minutes, with a time interval of 5 seconds. The density was calculated using both mass and volume of the filtrate. The equipment used are shown in Figure 2-4.

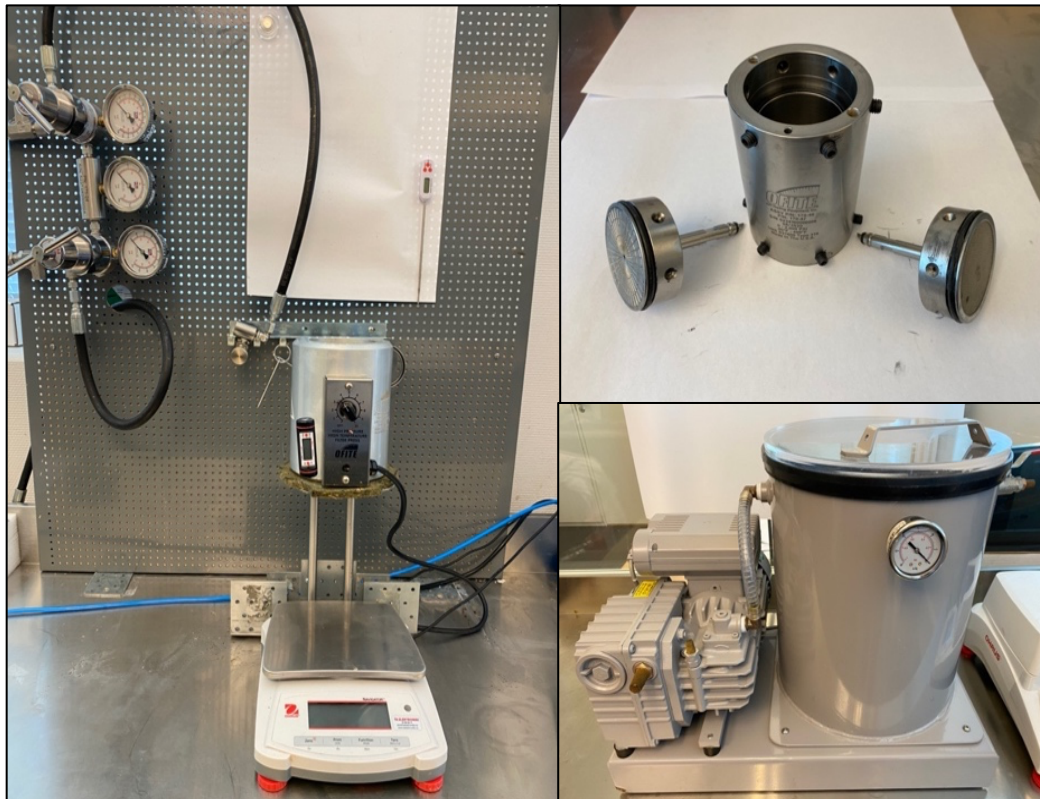


Figure 2-4: Ofite Filter Press HTHP 175 mL Double Capped to the left, fluid cell to the upper right, DVP EC.20-1 vacuum machine to the lower right.

Both soaked discs and filter papers were used to conduct fluid loss tests. Filter papers with pore throat openings of 11 and 20-25 μm were used. The procedure for fluid loss testing was the same as for the discs, except no soaking in freshwater and the applied differential pressure was 500 psi (3.5 MPa). Discs with the sizes used in the following experiments are shown in Figure 2-5.

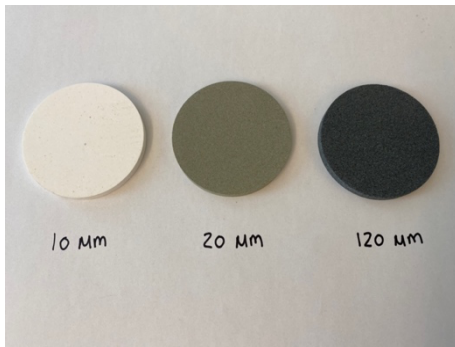


Figure 2-5: Ceramic disc used for fluid loss tests.

2.4.2. Reverse flow and filter cake removal

To remove the filter cake, a setup shown in Figure 2-6 was used, allowing water to flow through the disc in opposite direction of the drilling fluid flow. More details on the experimental setup are described by Klungtvedt and Saasen (2022c).

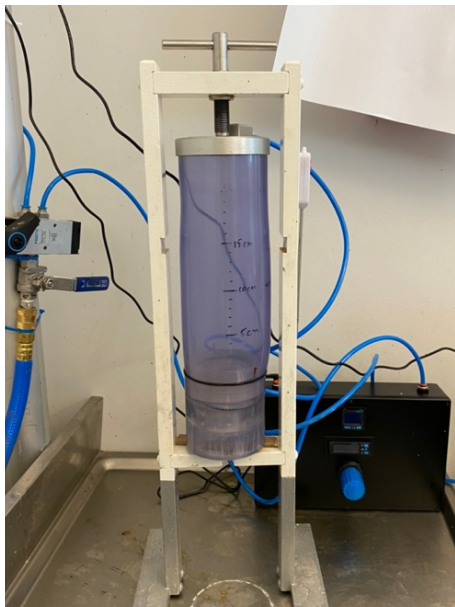


Figure 2-6: Transparent cylinder, Festo Pressure regulator LRP-1/4-2.5 and LRP-1/4-0.25, Festo Pressure Sensor SPAN-P025R and SPAN-P10R, Fest Flowmeter SFAH-10U.

After a fluid loss test, the disc was placed in the cylindrical cell with the filter cake facing downwards. 1 L of boiled freshwater was poured into the cylinder. Differential pressure was applied, forcing water through the disc, and removing the filter cake with varying degree of success. After reverse water flow, the disc was pictured to document the ability of filter cake removal. When parts of the filter cake were stuck on the disc, a sharp object was used to remove remaining parts.

2.4.3. Disc mass

To investigate if fluid invasion gave any settling of particles, the Ohaus Moisture Analyzer shown in Figure 2-7 was used to measure disc mass. To ensure the disc did not contain any water, the moisture analyzer dried the disc at 105 °C until change in weight was stable for 60 seconds, with a margin of 1 mg. The first measuring was done in the beginning of the fluid loss test procedure, before soaking the disc in water. To find if any change in disc mass occurred due to fluid invasion, a new measuring of disc mass was done after filter cake removal.



Figure 2-7: Ohaus MB120 Moisture Analyzer.

2.4.4. Permeability

To investigate how invasion of different fluids had an impact on the permeability, measurements were done before fluid invasion and after filter cake removal. The remaining of the original permeability is the retained permeability value. In this thesis, only permeability to air was measured, hence it is crucial to remove any potential moisture inhibiting flow through the pores. As the moisture analyzer from Figure 2-7 is supposed to remove potential moisture, the permeability measurements were conducted after weighing the disc, both before and after fluid loss tests. As temperature may impact the permeability measurements, the discs were cooled to air temperature before the permeability was measured, to create as similar testing conditions as possible. The disc was then placed in the cell shown in Figure 2-8 where pressure was applied, and the air temperature was measured. The flowrate at four different pressures was conducted. Calculation of permeability is shown in Appendix A.



Figure 2-8: Festo Pressure regulator LRP-1/4-2.5 and LRP-1/4-0.25, Festo Pressure Sensor SPAN-PO25R and SPAN-P10R, Festo Flowmeter SFAH-10U, cell for disc insert.

2.4.5. Fluid filtrate analysis

A series of tests were conducted to investigate the amount polymers in the respective filtrates. The refractive index, hereby referred to as BRIX, was measured using a sucrose refractometer. As the particles may experience sag, the filtrate was turned upside down a few times as an attempt to obtain a more even distribution. A small amount of the filtrate was applied to the refractometer using the pipette, and a BRIX reading was conducted. This procedure was repeated 3-5 times to verify consistent results, and an average value was used if small variations occurred.

Further, the filtrate was diluted 1:5 with water, and a small amount was poured into the plastic cup of the Eutech Expert CTS measuring device. The turbidity, salinity and conductivity readings were conducted for the diluted filtrates, as the concentration of the original filtrate could possibly be out of range of the equipment. The equipments used to conduct measurements of the filtrate content are shown in Figure 2-9.



Figure 2-9: Hanna Instruments Sucrose Refractometer HI 96801 to the left, Eutech Expert CTS to the right.

2.5. Pressure logging on tapered disc with differential pressure > 1000 psi (6.9 MPa)

The Permeability Plugging Apparatus shown in Figure 2-10 has a system testing limit of 5000 psi (34.5 MPa) and was used to measure the sealing pressure and necessary pressure to lift off the filter cake for LCM pills. Discs with tapered fractures were inserted before fluid was added, and the cell was heated to 90 °C to represent a reservoir temperature. The fractures were created by half-moon shaped steel units with different tapering shown in Figure 2-11, creating a larger inlet than outlet size of the fracture. For testing, three different outlet sizes were used: 900, 2500

and 3400 μm . Pressure tests were then conducted with the purpose of obtaining the highest pressure possible up to around 4500 psi (31 MPa). The pressure was logged digitally and could be applied either by a hydraulic pump or a gas source providing about 120 psi (0.83 MPa).

After testing of the sealing pressure was done, the tapered disc housing with filter cake was inserted upside down in the cell, before adding brine water with 10 lbs/bbl NaCl. A similar procedure as for sealing pressure testing was then used to measure the necessary pressure to lift of the filter cake.



Figure 2-10: Permeability Plugging Apparatus to the left, main parts of the insert in the middle, pressure and logging device to the right.

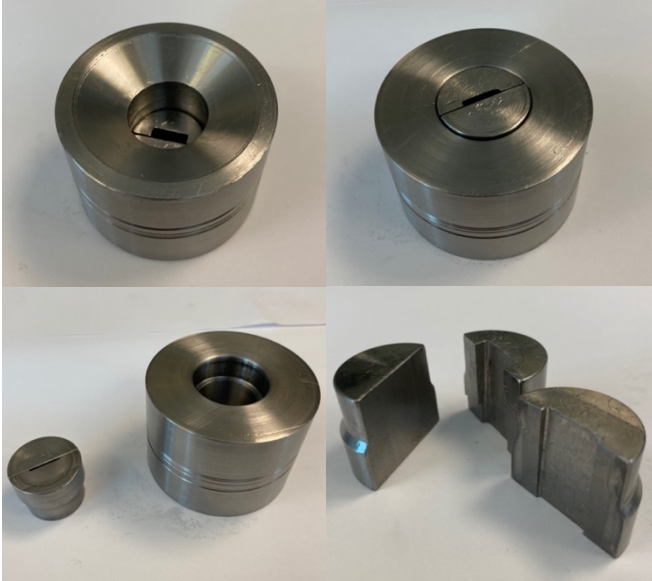


Figure 2-11: Tapered discs used for pressure testing and filter cake removal.

3. Experimental work, results and discussion

This part consists of four sections. The first section presents how mechanical wear impacts particle size distribution and fluid loss. In section two it was investigated how addition of CaCO₃ and fibers impacts rheology and sealing properties of the base fluid, while section three presents the impact of changing the starch type in the base fluid. Section four presents how different LCM pills impact sealing capacity and filter cake clean-up. Table 3-1 lists different samples that were tested in these experiments. Detailed information about the conventional drilling fluids and LCM pills is shown in Appendix B.

Table 3-1: Overview of fluids used for samples in the thesis.

Sample number	Referred to as:	Name of fluid recipe in Appendix B
1	Base	Fluid 1
2	Base + Additive 1	Fluid 2
3	Base	Fluid 3
4	Base with 9 μm CaCO ₃	Fluid 5
5	Base + Additive 2	Fluid 4
6	Base with 9 μm CaCO ₃ + Additive 2	Fluid 6
7	Base with 9 μm CaCO ₃ + Additive 4	Fluid 6
8	Base + Additive 3	Fluid 7
9	CPS Base	Fluid 8
10	CPS Base + Additive 2 (XC 1,5)	Fluid 8
11	CPS Base + Additive 2 (XC 1,3)	Fluid 9
12	Pill 1	-
13	Pill 2	-
14	Pill 3	-
15	Pill 4	-
16	Pill 5	-

3.1. Degradation of PSD

In this section, Sample 1 and 2 was used to evaluate how the resistance towards particle degradation affects the sealing capability of the fluid.

3.1.1. Effect of mechanical degradation on CaCO₃

The diagram in Figure 3-1 shows how hot-rolling with a steel rod affected the distribution of particles for *Base*, Sample 1, which contains CaCO₃ particles. The purpose of the steel rod is to simulate mechanical wear in the well, as explained in section 2.1. Before hot rolling (BHR), the particles were distributed up to 150 μm, where 79.3 % were smaller than 53 μm. After hot rolling (AHR), 99.8 % of the particles were smaller than 53 μm. The almost total degradation of particles larger than 53 μm may indicate that the larger particles were not able to withstand the mechanical and thermal wear from hot-rolling with a threaded steel rod. This may indicate that the sealing ability will rapidly deteriorate as the particles grind down due to circulation during drilling.

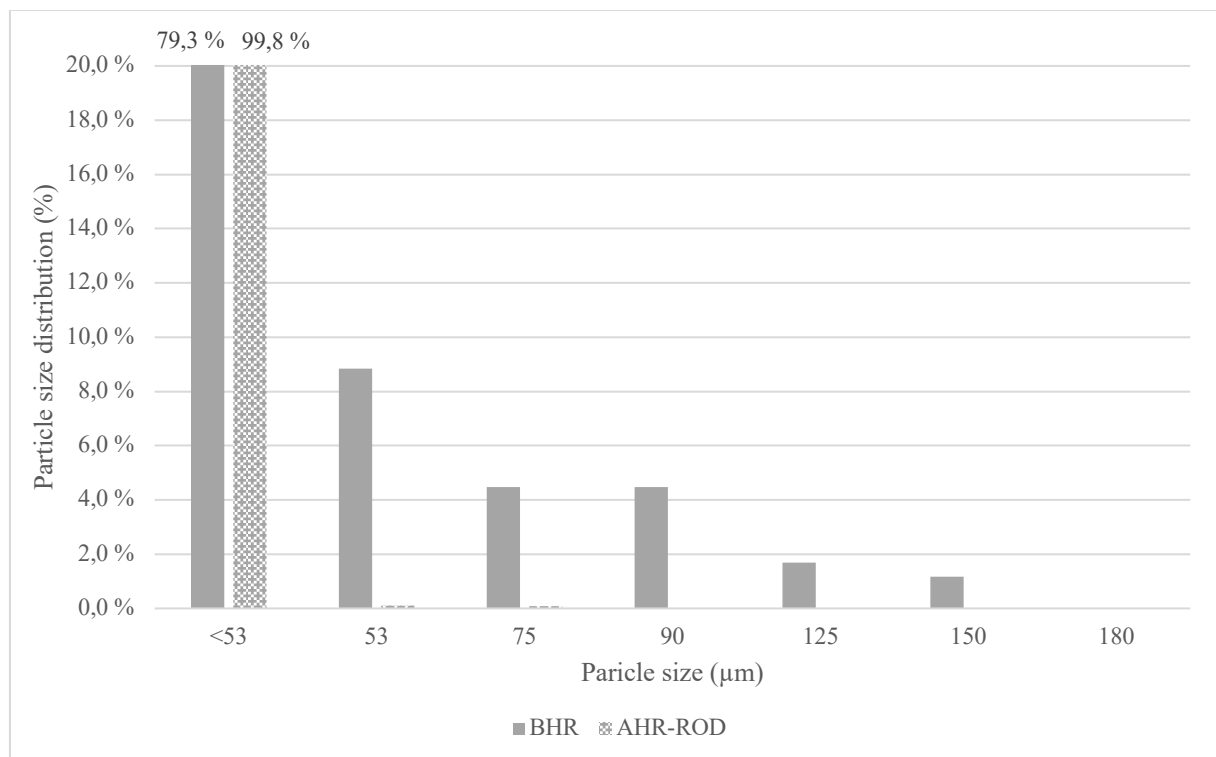


Figure 3-1: PSD of Sample 1, a fluid with CaCO₃ up to 53 μm before (BHR) and after hot-rolling using grinding rod (AHR-ROD).

3.1.2. Effect of mechanical degradation on fiber

Figure 3-2 shows the distribution of particles for *Base + Additive 1*, Sample 2, before and after hot-rolling with a steel rod, to simulate mechanical wear. *Base + Additive 1* contains both CaCO_3 and cellulose-based fiber particles, therefore, to separately measure the PSD of Additive 1, all the CaCO_3 was $< 53 \mu\text{m}$. The fluid had a particle distribution up to at least $180 \mu\text{m}$ size BHR. The change in PSD due to hot-rolling was minimal and may indicate that Additive 1 was able to withstand the mechanical and thermal wear. There was only a 0.4 % increase in particles less than $53 \mu\text{m}$ because of hot-rolling, which is within the uncertainty of the measurement. The results from Figure 3-2 indicates that during circulation, *Base + Additive 1* will maintain its sealing ability.

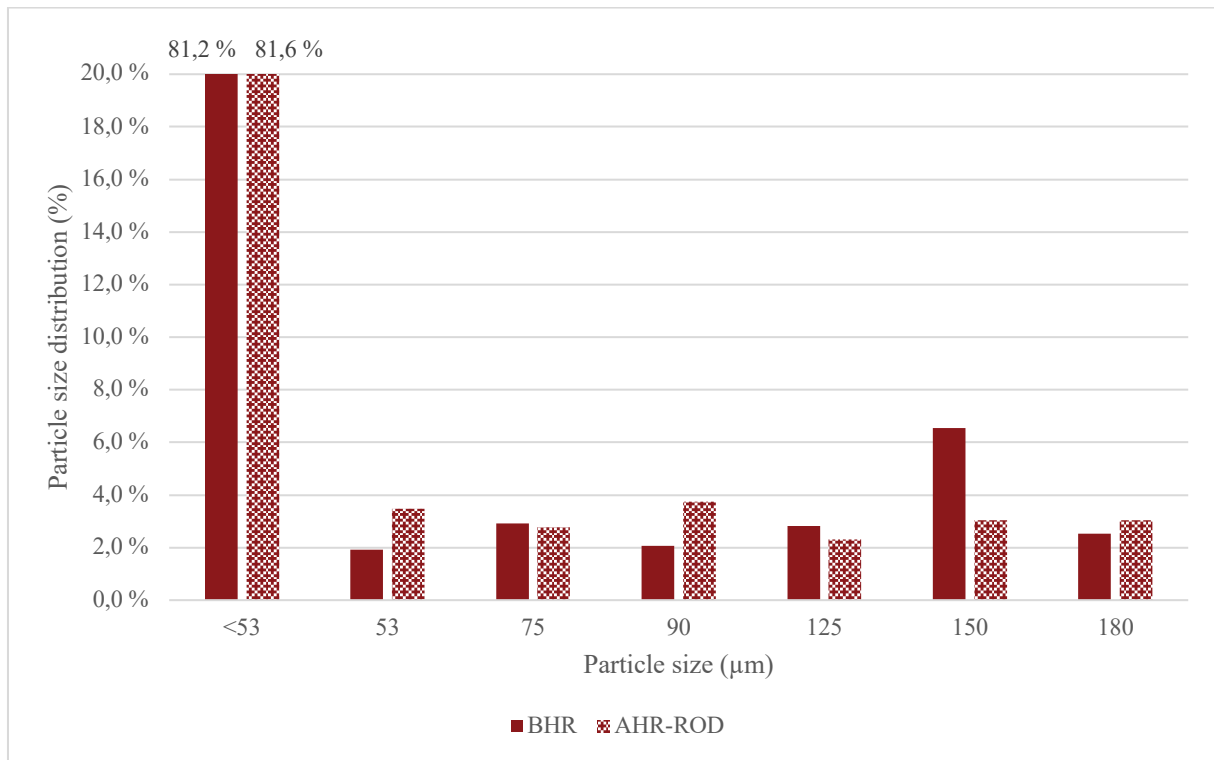


Figure 3-2: PSD of Sample 2, a fluid with CaCO_3 up to $23 \mu\text{m}$ and fiber (Additive 1) before (BHR) and after hot-rolling using grinding rod (AHR-ROD).

3.1.3. Effect on fluid loss

Figure 3-3 shows the fluid loss curves on a 120 μm disc for *Base* and *Base + Additive 1* AHR. *Base* resulted in total loss, even without the steel rod. The measured degradation in PSD for *Base* with rod may indicate that it would have resulted in total loss as well. Figure 3-1 shows that the fluid contained in excess of 20 % particles of 53 μm and larger BHR and practically zero AHR. The total fluid loss may therefore be explained by a significant degradation of the particles $> 53 \mu\text{m}$, i.e. particles larger than 44 % of the disc pore throat size, due to hot-rolling. However, the total loss could also be caused by an external factor and might not be a valid test, hence further test should be conducted before concluding. The fluid loss curve for *Base + Additive 1* is approximately the same with and without rod, with a fluid loss of about 15 mL after 30 minutes.

The significant difference in sealing capability of *Base* and *Base + Additive 1* may indicate that the ability to maintain the original PSD during hot-rolling impacts fluid invasion. To verify the consistency of the results, further tests should be conducted.

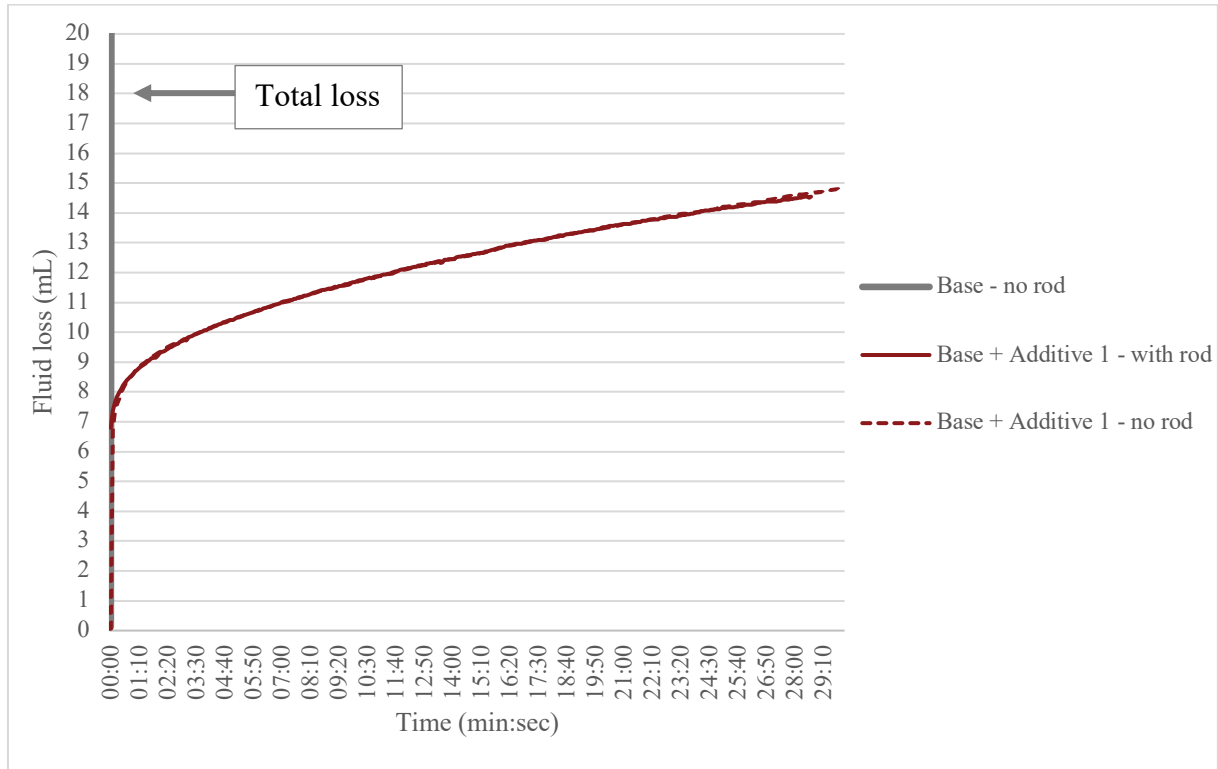


Figure 3-3: Fluid loss curves for fluid with only CaCO_3 (*Base - no rod*) and fluid with a combination of CaCO_3 and fiber both with grinding rod (*Base + Additive 2 - with rod*) and without grinding rod (*Base + Additive 1 - no rod*) on 120 μm discs with 1000 psi (6.9 MPa) differential pressure.

3.2. Different PSD compositions of CaCO₃ and the effect of adding fiber

The aim of this section is to present how different PSD compositions of CaCO₃ and addition of fiber effects viscosity, fluid loss, disc mass and permeability and fluid filtrate composition. Samples 3-7 was used to conduct the experiments in this section.

3.2.1. Viscosity parameters

Figure 3-4 shows the viscosity readings of base fluids with only CaCO₃ as LCM and with fibers and CaCO₃ as LCM with shear rates of 1000 and 300 reciprocal seconds. In an 8 ½” reservoir section, the shear rates are varying depending on the difference in diameter of the hole and the outer diameter (OD) of the pipe or bottom hole assembly (BHA). If the OD of the pipe or BHA is reduced, the annular volume is increased, thus resulting in lower shear rates. The highest shear rates in the section will therefore be for the pipe or BHA with the largest OD, which will result in shear rates around 300 (1/s). The viscosity profiles for the relevant range are shown in Figure 3-4 2).

As all fluids tested use the same type of xanthan gum (XC) polymer as viscosifier, with concentrations between 1.4 and 1.6 lbs/bbl, some variation in rheological properties can be expected. *Base* contained 1.5 lbs/bbl and *Base with 9 μm CaCO₃* contained 1.6 lbs/bbl of XC polymer. When fiber was added, the amount was reduced with 0.1 lbs/bbl for both fluids. As the data in Figure 3-4 represents shear stress in pascal and shear rate in reciprocal seconds, the slope of each fluids indicates thixotropic or shear thinning behavior.

Figure 3-4 a) shows that up to a shear rate of approximately 50 (1/s), both *Base* and *Base with 9 μm CaCO₃* showed almost identical viscosity readings BHR, where for the shear rates over 50 (1/s), *Base with 9 μm CaCO₃* showed slightly higher viscosity readings than *Base*. Hot-rolling resulted in slightly higher viscosity readings over 50 (1/s) for *Base*, while slightly lower viscosity readings over 340 (1/s) for *Base with 9 μm CaCO₃*. The difference in viscosity is within the uncertainty of the test.

Figure 3-4 shows that hot rolling of fluids with both fiber and CaCO₃ resulted in a slight increase in viscosity readings. These values are slightly higher than for fluids with only CaCO₃. This may be due to the fibers' ability to absorb water in a low salinity fluid and therefore

expand, resulting in a more viscous fluid. Alternatively, a lower concentration of xanthan gum may be used.

The viscosity readings for *Base* and *Base with 9 μm CaCO₃* AHR were similar for all shear rates. As were the viscosity readings of the three fluids with fiber and CaCO₃. This may indicate that distribution of CaCO₃ particles and type of fiber have little impact on viscosity after hot-rolling at 112 °C. Further testing with different types of fiber and PSD of CaCO₃ should be done before concluding.

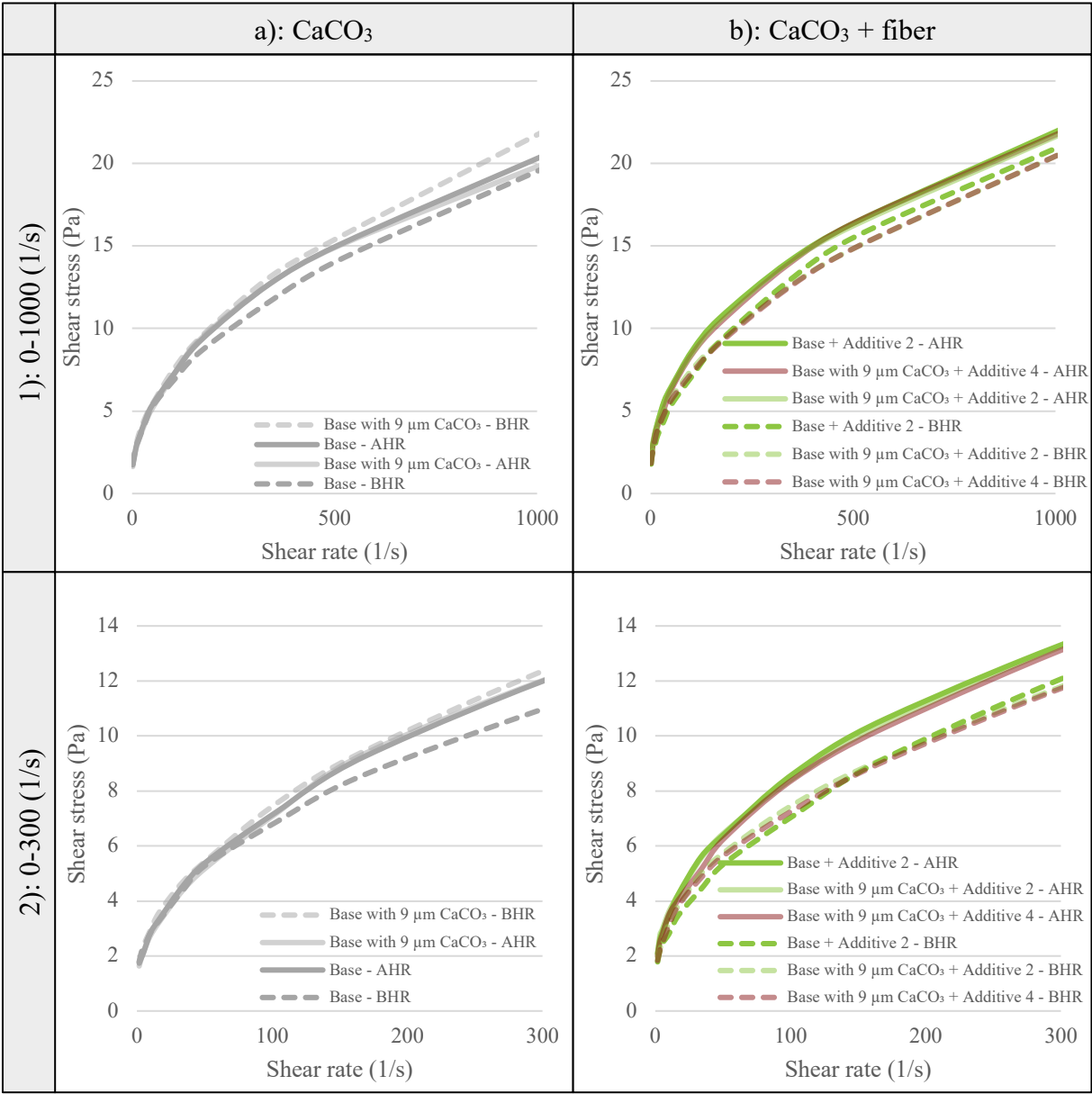


Figure 3-4: Viscosity measurements with shear rates in range 0-1000 (1/s) in 1) and 0-300 (1/s) in 2) of fluids with only CaCO₃ in a) and fluid with addition of fiber in b).

3.2.2. Fluid loss

Figure 3-5 shows the fluid loss in 30 minutes of testing on three different disc sizes (10, 20 and 120 μm). Fluids with only CaCO_3 is presented in a) to the left, with addition of different fibers in b) to the right.

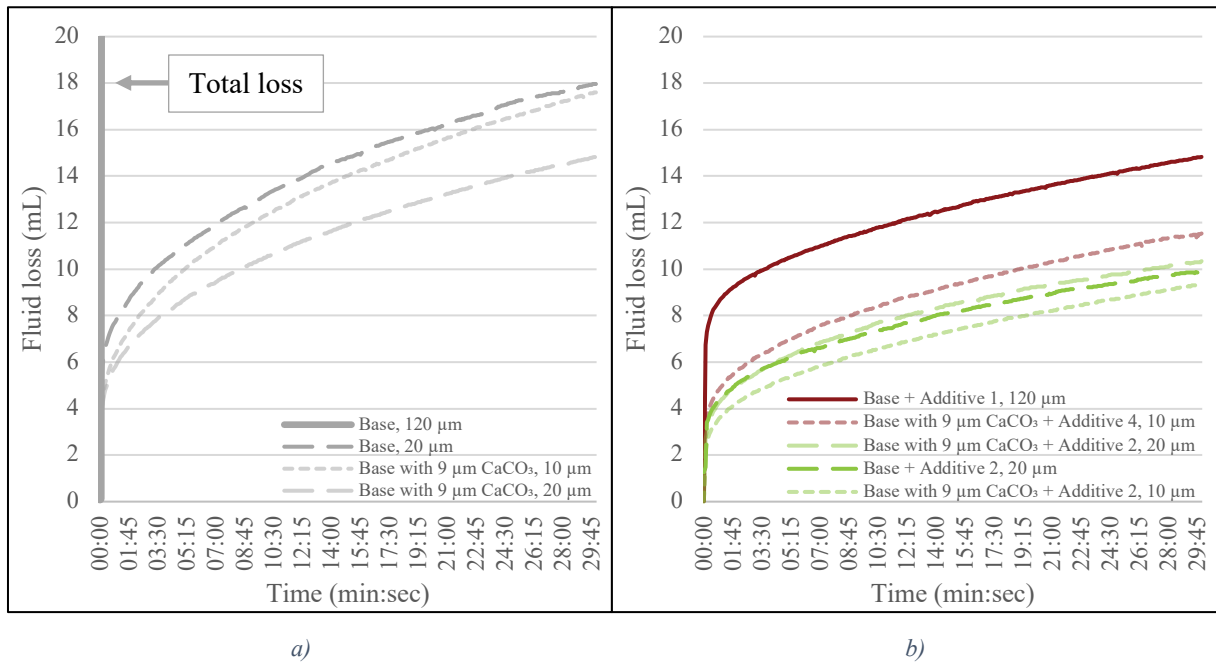


Figure 3-5: Fluid loss on 10, 20 and 120 μm discs for 30 minutes. Fluids with only CaCO_3 in a) and fluids with addition of fiber in b).

Figure 3-5 shows that *Base* was unable to create an adequate filter cake on a 120 μm disc, with total loss after a few seconds. On a 20 μm disc, *Base* resulted in a fluid loss of about 18 mL after 30 minutes. *Base with 9 μm CaCO_3* resulted in a slightly reduced spurt loss compared to *Base*, with approximately the same curve gradient afterwards, resulting in a 3.3 mL lower fluid loss after 30 minutes. The main difference between *Base* and *Base with 9 μm CaCO_3* is the CaCO_3 PSD, see Fluid 1 and 5 in Appendix B, where Fluid 5 contains equal amount of 9 μm and 50 μm CaCO_3 particles. The reduced fluid loss on 20 μm discs when replacing 10 lbs/bbl 50 μm CaCO_3 with 10 lbs/bbl 9 μm CaCO_3 , may indicate that changing the PSD of CaCO_3 , can impact fluid loss. However, due to few test data, this can not be concluded. *Base with 9 μm CaCO_3* on a 10 μm disc gave similar spurt loss as on the 20 μm disc, but with a higher fluid loss after 30 minutes. As the fluid loss on 10 and 20 μm discs were significantly lower than on a 120 μm disc, it may indicate that the sealing ability of fluids with $\text{CaCO}_3 < 53 \mu\text{m}$ as LCM will deteriorate with increasing formation permeability.

The curve for *Base + Additive 1* on a 120 μm disc in Figure 3-5 b), shows a spurt loss of about 8 mL before flattening out in an almost constant rate, resulting in a fluid loss of about 15 mL after 30 minutes. The curve shows a significant change from total loss with *Base* on 120 μm disc, even when the CaCO_3 concentration was reduced from 40 to 20 lbs/bbl (Fluid 2 and 4 in Appendix B). This may indicate that fibrous materials are more effective as LCM than CaCO_3 , but more test data should be conducted before concluding. On 20 μm discs, *Base + Additive 2* and *Base with 9 μm $\text{CaCO}_3 + Additive 2$* resulted in similar curves, with a fluid loss around 10 mL after 30 minutes. On a 10 μm disc, *Base with 9 μm $\text{CaCO}_3 + Additive 4$* resulted in a fluid loss of about 11.5 mL after 30 minutes. When switching Additive 4 with Additive 2, the curve for the 10 μm disc shows a similar gradient and lower spurt loss, thus a lower fluid loss after 30 minutes. This curve shows the lowest spurt- and 30-minute fluid loss among the conducted tests.

Figure 3-5 shows that combining fibers and CaCO_3 as LCM gives significantly lower fluid loss after 30 minutes for both 10, 20 and 120 μm disc than when using only CaCO_3 . The slope gradient after spurt loss on the 10 and 20 μm disc tests are also smaller for the fluids with a combination of fiber and CaCO_3 compared to only CaCO_3 . The smaller slope gradient and lower fluid loss may indicate that the fiber particles help create a less permeable filter cake, that reduces invasion of fluid into the formation.

3.2.3. Disc mass and permeability

Figure 3-6 shows the disc mass increase after fluid invasion and retained permeability (the percent of the original permeability) after filter cake removal, for three different disc sizes (10, 20, 120 μm). Fluids with only CaCO_3 is presented in a) to the left, with addition of different fibers in b) to the right. The absolute differences in disc mass are very small and may be within the range of test uncertainty.

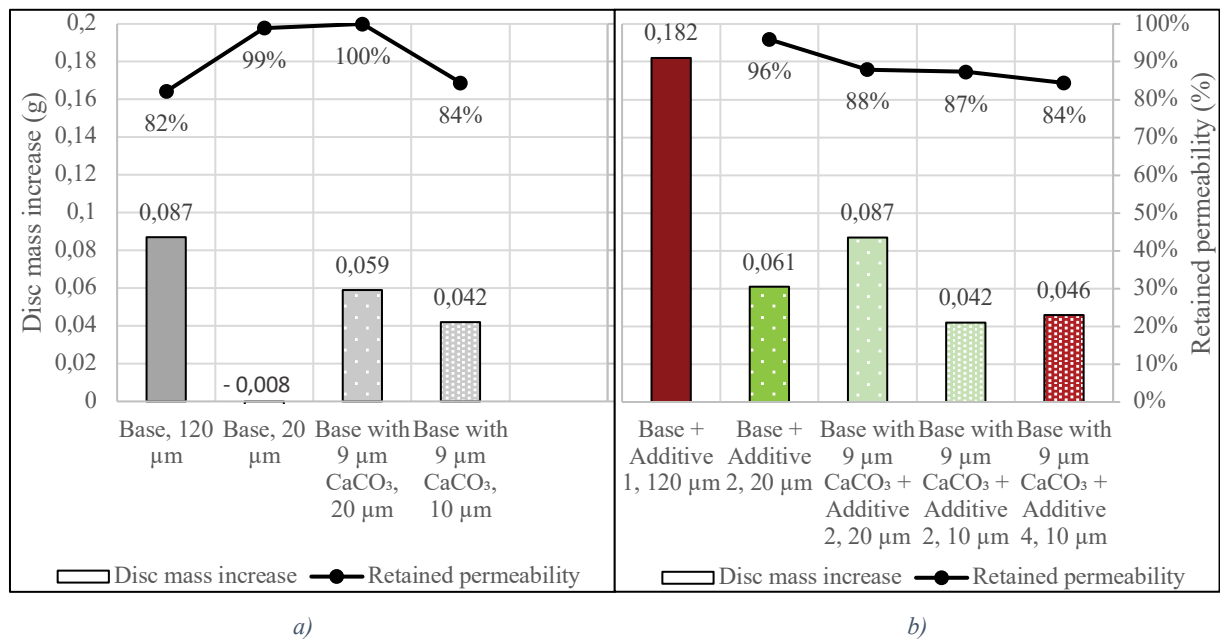


Figure 3-6: Disc mass increase and retained permeability of 10, 20, and 120 μm discs. Fluids with only CaCO_3 in a) and fluids with addition of fiber in b).

In Figure 3-6 a) the 120 μm disc with *Base* experienced a mass increase of 0.087 g and a retained permeability of 82 %. However, this permeability measurement may not be representative for formation damage, as the particles in a total loss case could migrate deeper into the formation. The low disc mass increase may indicate that particles were too small to get stuck in the disc. *Base* on 20 μm disc resulted in 99 % retained permeability and a mass increase of -0.008 g. As a negative mass increase value is not realistic, it is reasonable to assume that the change is due to test uncertainty. *Base with 9 μm CaCO_3* on a 20 μm disc gave total retained permeability and a disc mass increase of 0.059 g. When applied on a 10 μm disc, *Base with 9 μm CaCO_3* resulted in a mass increase and retained permeability of 0.042 g and 84 % respectively. The overall results for fluids with only CaCO_3 , show a disc mass increase and reduced permeability less than 0.1 g and 20 % respectively, which may indicate that CaCO_3 as LCM has low damaging effect on the formation, regardless of PSD of CaCO_3 .

As for the tests with only CaCO_3 as LCM, all tests with both fibers and CaCO_3 in Figure 3-6 b), except on 120 μm disc, resulted in mass increase and permeability decrease of less than 0.1 g and 20 % respectively. Permeability measurement was not conducted on a 120 μm disc with *Base + Additive 1*, but the results show a disc mass increase of 0.182 g. This is about 0.1 g larger than *Base*, but as the disc only increased by 0.36 % of the original disc mass of 50.402 g, the increase is still relatively small with regards to formation damage. *Base + Additive 2* on a 20 μm disc gave a retained permeability of 96 % and a mass increase of 0.061, while *Base with 9 μm CaCO_3 + Additive 2* resulted in lower retained permeability as well as a small increase of the 20 μm disc mass. Using *Base with 9 μm CaCO_3 + Additive 2* on a 10 μm disc, gave a disc mass increase and retained permeability of 0.042 g and 87 % respectively, and when switching Additive 2 with Additive 4, no significant change regarding formation damage were observed.

The results in Figure 3-6 shows no significant signs that changing PSD of CaCO_3 is impacting formation damage. However, more tests should be conducted to verify these observations. The overall results indicates that the fluids with only CaCO_3 and those with a combination of CaCO_3 and fibers as LCM, produce results with high degree of retained permeability and low mass increase, and hence present interesting alternatives for a non-damaging reservoir drilling fluid.

As CaCO_3 and the fibrous materials are acid soluble, application of an acidic breaker may reduce the mass increase and permeability change even more. As the current results show low formation damage, further evaluation should be done to assess whether such application is necessary or not. However, such items are not discussed in this thesis.

3.2.4. Fluid filtrate

A method for estimating the amount of polymers in the filtrate described by Klungtvéd and Saasen (2022d) was used to investigate how the filter cakes had an impact on the content of the filtrate. Filter papers with pore throat openings around the discs size was used with the purpose of representing a similar formation as the disc. In Figure 3-7, the area of the bubbles represents the multiple of the fluid loss and the refractive index (BRIX) value, which is reflecting the absolute volume of polymers. Fluids with only CaCO₃ is presented in a), and fluids with addition of fibers in b). The results from testing on filter papers and discs are shown in 1) and 2) respectively.

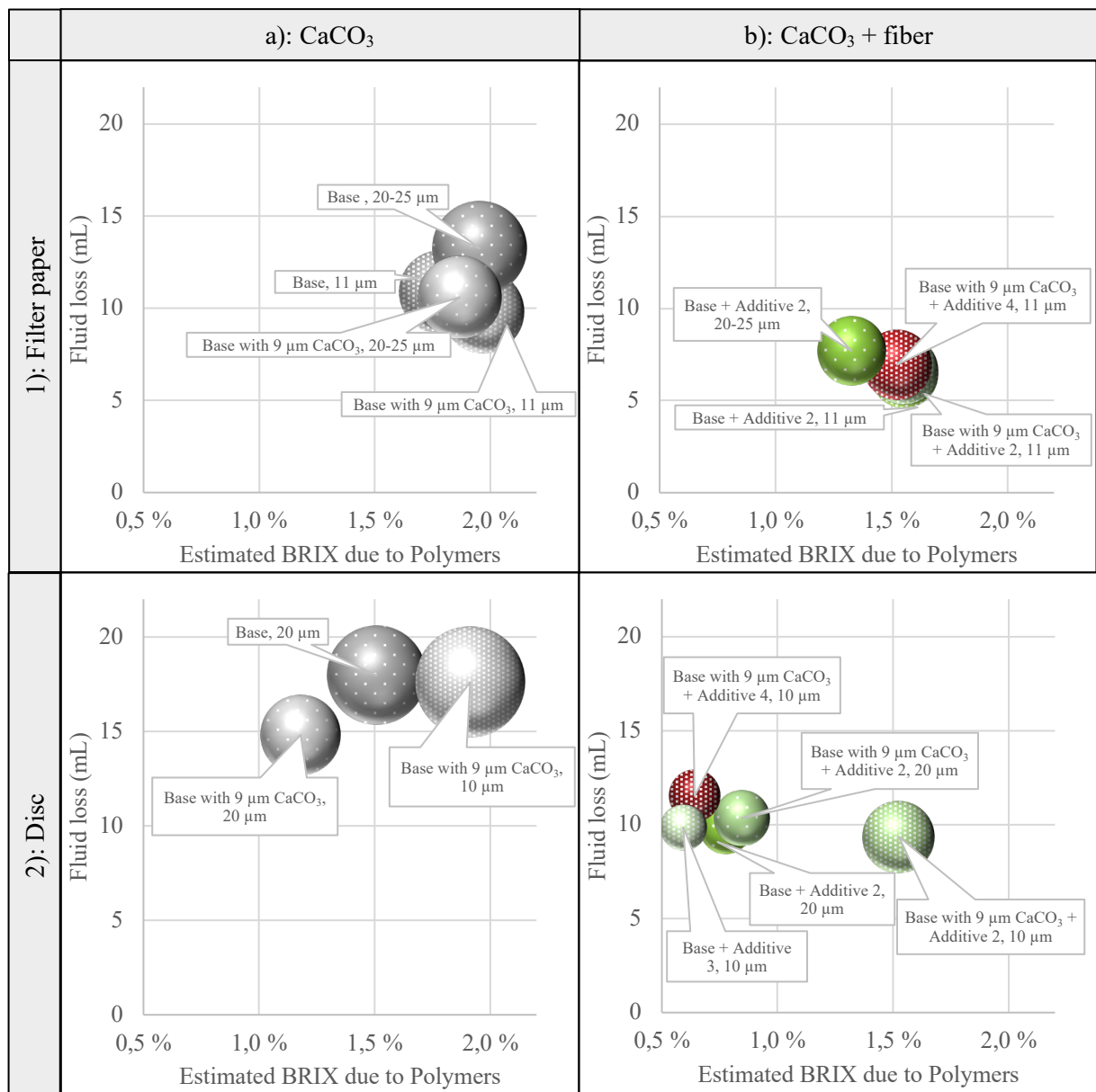


Figure 3-7: Amount polymers in the fluid filtrate from 11 and 20-25 μm filter paper tests (500 psi) in 1) and 10 and 20 μm disc tests (1000 and 750 psi) in 2). Fluids with only CaCO₃ in a) and fluids with addition of fiber in b).

For the fluids with only CaCO₃ as LCM, the results on filter paper indicated low variation in polymer concentration regardless of the size of the filter paper. On discs, the polymer concentrations were slightly more variable. When comparing the absolute volume from disc testing with the equivalent filter paper tests, the results show slightly increased values for *Base* and *Base with 9 μm CaCO₃* on 20 μm disc. *Base with 9 μm CaCO₃* on 10 μm disc resulted in an almost doubled volume of polymers. As the disc tests were conducted with higher applied differential pressure, this may indicate that for fluids with only CaCO₃, increased pressure reduces the ability to prevent polymers escaping through the filter cake.

As for the fluid with only CaCO₃, the results with both CaCO₃ and fibers show low variation in polymer concentration on filter paper tests, and slightly more variable concentrations for disc tests. For fluids with both CaCO₃ and fiber, comparing the absolute volume from disc testing with equivalent filter paper tests resulted in a slightly higher value on 10 μm disc for *Base with 9 μm CaCO₃ + Additive 2*. The other tests resulted in a reduced absolute volume for discs compared to filter paper, possible due to polymers being deposited in the discs, as the discs are porous and thicker than the filter papers. When using fluids with CaCO₃ and fiber as LCM, Figure 3-7 b) shows an overall reduction in both absolute volume and polymer concentration for both filter paper and disc tests compared to only CaCO₃ as LCM. This may indicate that fibers have a better ability to bind polymers in the filter cake. The results in Figure 3-7 may also indicate that there is no uniform behavior by using different PSD of CaCO₃.

3.3. Effect of changing starch type

To this point, a base fluid with modified starch has been used. The scope of this section is to investigate the effect of changing from modified starch to crosslinked potato starch (CPS). The grey color represents fluids with only CaCO₃ as LCM, and the green color represents fluids with both CaCO₃ and fiber. Sample 4, 6, 9, 10 and 11 are used in this section.

3.3.1. Viscosity parameters

Figure 3-8 shows the viscosity profiles for fluids with CPS in a) and fluids with modified starch in b). The fluids with CPS resulted in larger variation in viscosity profiles and higher shear stress readings compared to fluids with modified starch. BHR, the two *CPS Base + Additive 2* fluids had similar viscosity readings for the range up to approximately 100 (1/s), before the results show a slight difference in viscosity, possibly due to different XC polymer concentrations. AHR the viscosity readings were similar.

Both fluids with CPS and modified starch resulted in consistently lower viscosity readings for fluids with only CaCO₃, than fluids with both CaCO₃ and fibers. Hot-rolling resulted in lower viscosity readings for all CPS fluids, and higher readings for fluids with modified starch. This opposite reaction on viscosity profiles due to hot-rolling, may indicate that using CPS instead of modified starch, reduced the ability to maintain the viscosity when exposed to the temperature of 112 °C. Hence, this may not be a suitable alternative for a reservoir drilling fluid. However, different types and concentrations of polymers may also contribute to the viscosity variations.

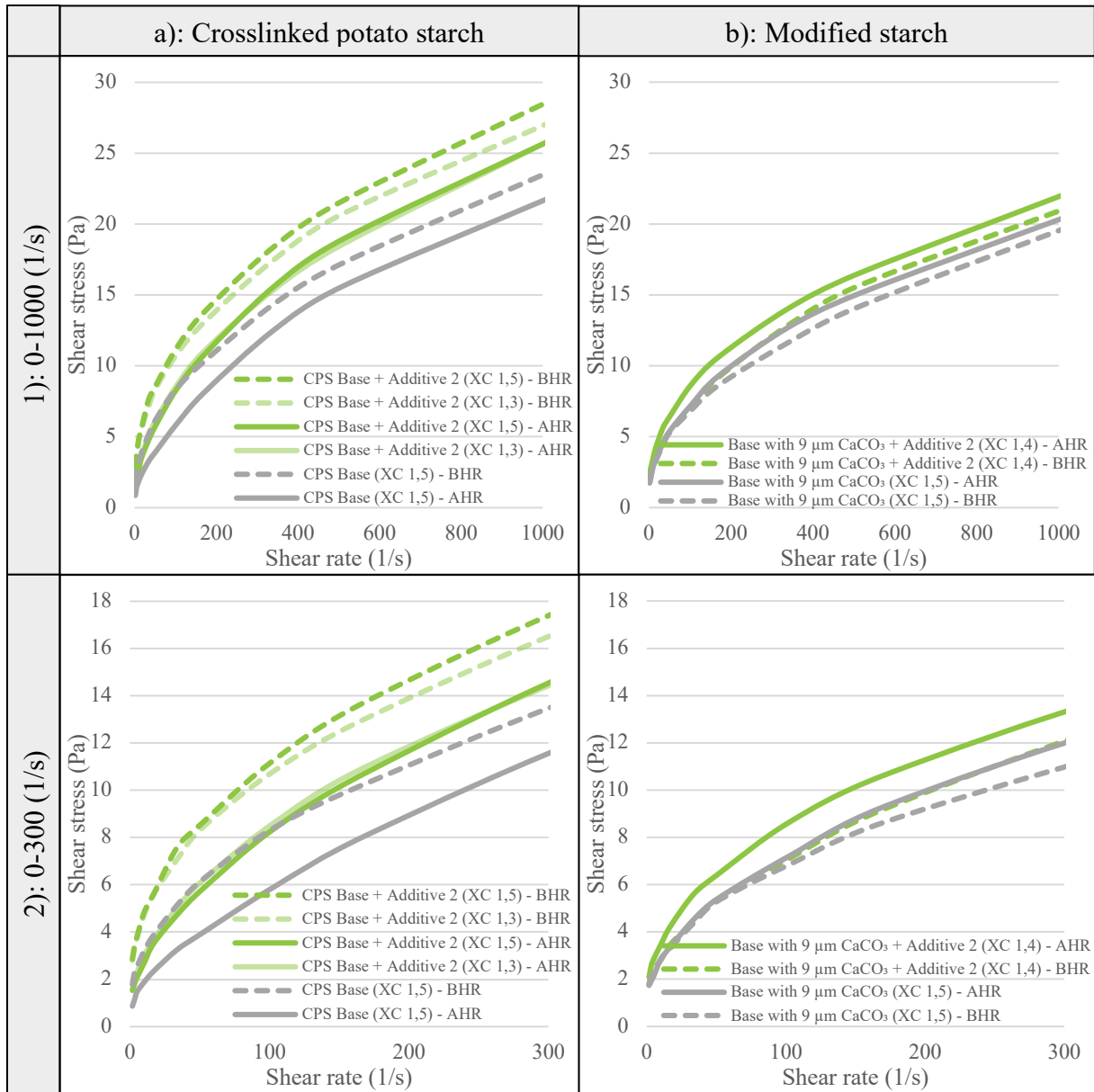


Figure 3-8: Viscosity measurements with shear rates in range 0-1000 (1/s) in 1) and 0-300 (1/s) in 2) of fluids with crosslinked potato starch in a) and fluids with modified starch in b).

3.3.2. Fluid loss

Both modified- and crosslinked potato starch has the purpose of acting as filtration control in the fluid. As the respective fluids are designed to have similar properties, similar fluid loss curves could be expected. Figure 3-9 shows how changing the modified starch with the CPS effected the fluid loss curves.

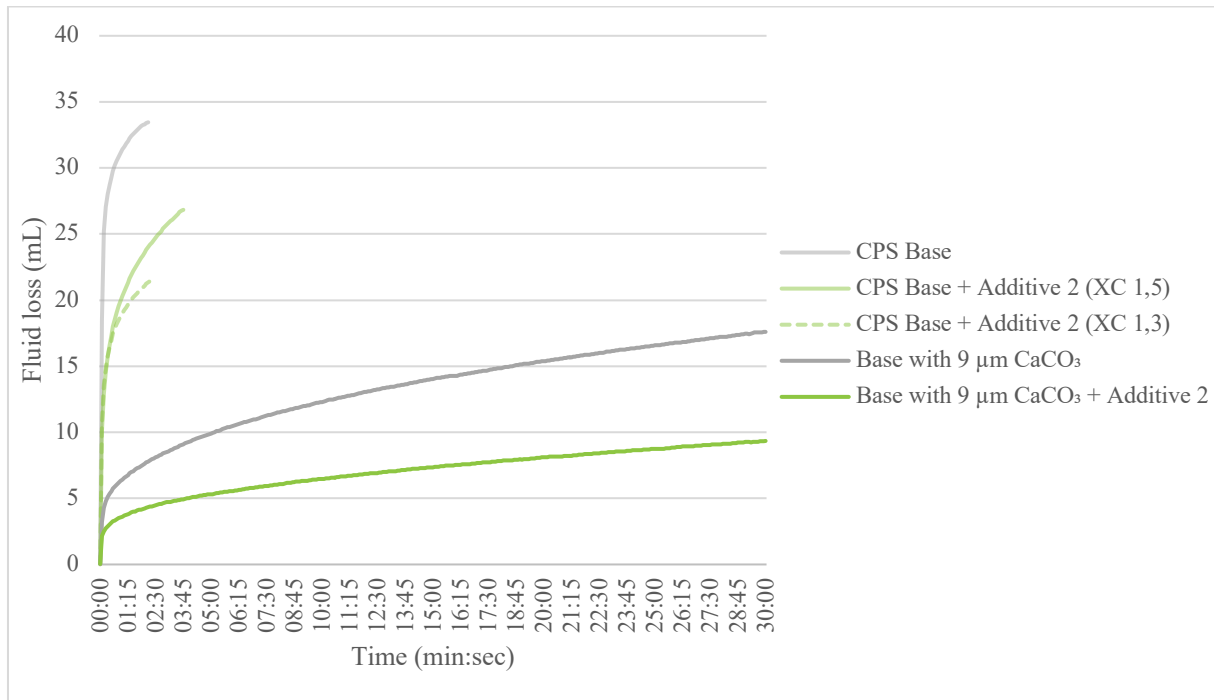


Figure 3-9: Fluid loss in 30 minutes for fluids with crosslinked potato starch and fluids with modified starch on 10 μm discs.

The results show a significant difference in spurt loss for the fluids with CPS and modified starch. After two minutes the fluid loss of *CPS Base* and *CPS Base + Additive 2 (XC 1.5)* was 25.7 and 19.4 mL higher respectively, compared to *Base with 9 μm CaCO₃* and *Base with 9 μm CaCO₃ + Additive 2*. CPS fluids formed smooth, slightly thicker filter cakes than the modified starch fluids, which possibly can increase the risk of getting stuck while drilling. The filter cakes are shown in Appendix D. As the CPS fluids have no data after four minutes, no comparison of the fluid loss increase after 30 minutes can be done. However, the large difference in fluid loss after two minutes may indicate that the respective modified starch had a better sealing ability, hence seems to be better suited as filtrate control for a reservoir drilling fluid used in a section of 112 °C.

3.3.3. Disc mass and permeability

Figure 3-10 shows the results of disc mass increase and retained permeability for fluids with modified starch and fluids with CPS.

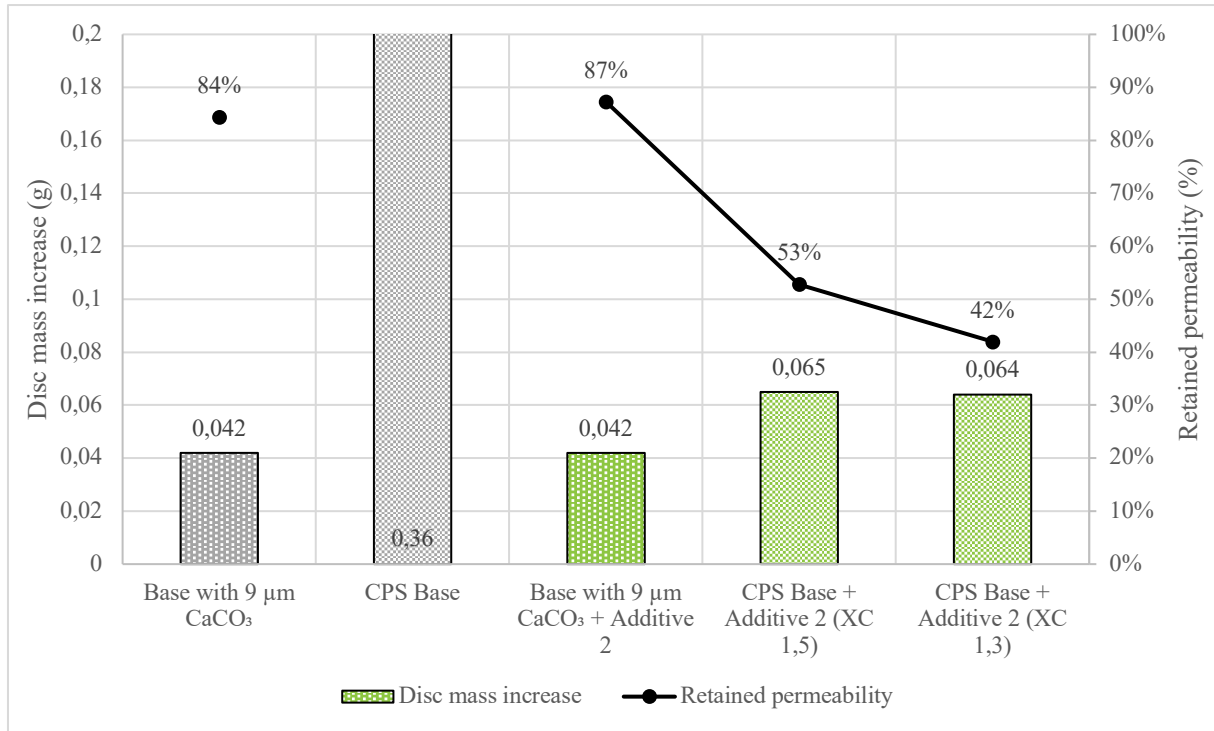


Figure 3-10: Disc mass increase and retained permeability for fluids with crosslinked potato starch and fluids with modified starch on 10 μm discs.

CPS Base resulted in a disc mass increase about 8.6 times larger than *Base with 9 μm CaCO_3* . During reverse flow with water and air pressure, the *CPS Base* disc fractured, hence no permeability measurement was conducted after filter cake removal, and no retained permeability was calculated. The higher mass increase for *CPS Base* may be due to some water seeping through the fractures instead of the pores during filter cake removal, thus this test may not be representative.

For the fluids with CaCO_3 and fiber as LCM, the results show a slightly higher disc mass increase and a significant decrease in retained permeability for the *CPS Base + Additive 2* fluids compared to *Base with 9 μm CaCO_3 + Additive 2*. During filter cake removal from the discs used for the *CPS Base + Additive 2* fluids, the water slowly seeped through the discs with a rate of about 4.2 cm^3/s . The low disc mass increase, relatively high spurt loss, and low flow rate

may indicate that instead of working as filtration control, the starch polymers seeped through the filter cake and plugged the disc, thus resulting in retained permeability values below 50 %. *CPS Base* includes the same starch polymers, thus the fractured disc may be explained by the applied air pressure forcing the water through the reduced permeability disc. Due to only one data point, further testing should be conducted before concluding. The overall permeability- and disc mass results from this section indicates that the CPS fluids are not suited for use in reservoir sections where temperature reaches 112 °C, as they can cause significant formation damage.

3.4. Effect of using CaCO₃ in LCM pills

To this point, the function of drilling fluids on low permeable reservoir zones have been discussed. When drilling in a reservoir, fractures can be encountered which can have a significant increase in permeability. They can be natural fractures or induced by drilling. The scope of this section is to investigate the ability to remove the filter cake after sealing a fracture with different LCM pills. The results of this section were conducted with samples 11-15, where *Pill 1* only contains CaCO₃ as LCM and is designed as a self-sealing pill. *Pill 2-5* are designed as squeeze pills, where the purpose is to de-fluidize quickly, so that the particles may form a bridge across the fracture. *Pill 3* and *5* only contains fibers as LCM, while *Pill 2* and *4* are equivalent to *Pill 3* and *5* with addition of CaCO₃.

3.4.1. Differential sealing pressure

Five different LCM pills were tested to measure the sealing pressure up to approximately 4500 psi (31 MPa), as the system testing limit is set to 5000 psi (34.5 MPa). The tests were conducted on tapered discs with fracture sizes of 900, 2500 and 3400 μm. Figure 3-11 presents the maximum measured sealing pressure for different LCM pills with CaCO₃, fibers, and a combination of CaCO₃ and fibers. The indicators represent the sustainable hold pressure (SHP; over a 60 second period) unless marked as peak hold pressure (PHP; over a 10 second period), and the white fill color represents presence of CaCO₃ in the fluid.

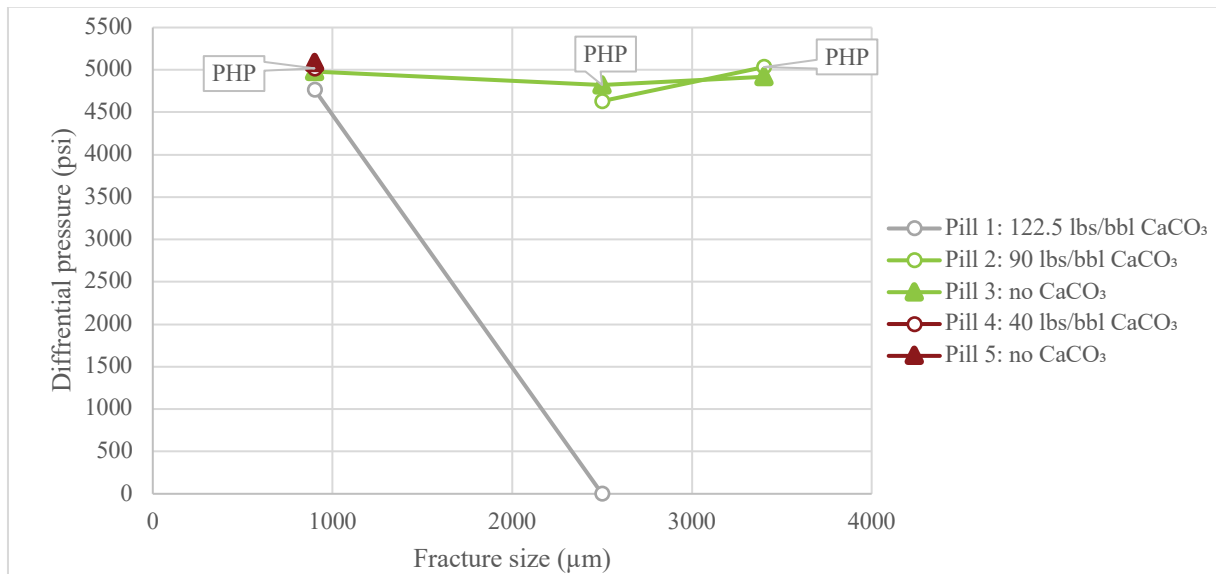


Figure 3-11: Maximum measured sealing pressure on tapered discs with different fracture sizes for LCM pills containing only CaCO₃ (Pill 1), only fiber (Pill 3 and 5) and both CaCO₃ and fiber (Pill 2 and 4). White indicators represent CaCO₃ in the formulation.

The results show a SHP for *Pill 1, 3 and 5* and a PHP for *Pill 4* over 4500 psi (31 MPa) when applied on a disc with 900 μm fracture width. It was assumed that the size of the particles for the cellulose-based LCM materials in *Pill 4* and *5* were too small compared to the fracture width, and thus would not be able to seal the disc with 2500 μm fracture width. Hence, these tests were not conducted. *Pill 1* was not able to seal the disc with fracture width of 2500 μm , possibly due to too small CaCO_3 particles. For further knowledge of the sealing capability of *Pill 1*, it would be desirable to test on a fracture width between 900 and 2500 μm . *Pill 2* and *3* was able to seal 2500 and 3400 μm fracture width with a pressure over 4500 psi (31 MPa).

As *Pill 2-5* were designed as squeeze pills, water was expected to quickly seep through the fracture. When air pressure of around 120 psi (0.83 MPa) was applied, pills without CaCO_3 were de-fluidized, while pills with CaCO_3 were not. When observing the sealed discs after pressure testing, it looked like the pills with CaCO_3 had only sealed the fracture. The debris on top of the fracture was wet. In contrast, pills without CaCO_3 formed large plugs on top of the fracture. The plugs were hard and dry in the middle. Pictures of the sealed fractures are attached in Appendix C.

The results may indicate that the CaCO_3 particles could regulate the de-fluidization of the LCM pills, and thus improve control of the filter cake structure and diameter of the wellbore. This could possibly help controlling the risk of getting stuck after applying an LCM pill.

3.4.2. Lift off pressure

To measure the ability of the pills to be removed from the formation, an experimental method was applied. The tapered disc housing was inserted the opposite way in the cell than for the sealing pressure tests, and both air pressure and hydraulic pressure were applied to remove the filter cake. The necessary pressure to force 350 mL brine with 10 lbs/bbl NaCl through the fracture is shown in Figure 3-12, where the white indicators are representing content of CaCO₃.

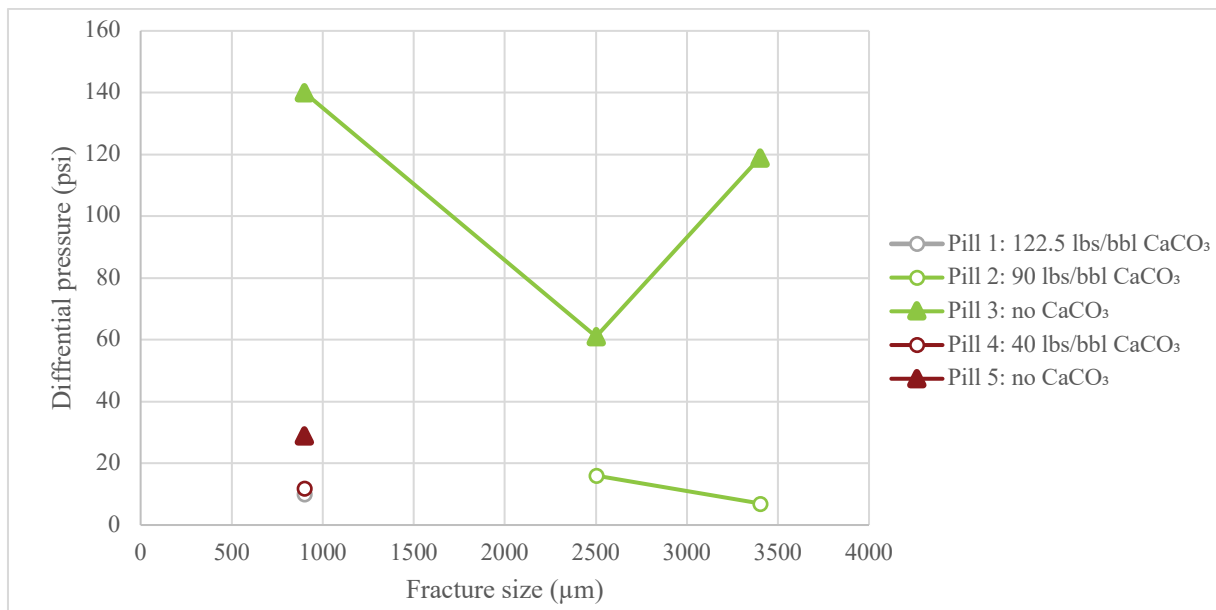


Figure 3-12: Pressure needed to remove the filter cake enough for brine to flow through the fracture for LCM pills containing only CaCO₃ (Pill 1), only fiber (Pill 3 and 5) and both CaCO₃ and fiber (Pill 2 and 4). White indicator represents addition of CaCO₃.

The results show that the pressure needed for brine to flow through the fracture was consistently lower for pills with CaCO₃ compared to pills without CaCO₃. After flowing of brine, a high number of particles was observed in the fracture for *Pill 3* regardless of the fracture width. Testing with *Pill 2* resulted in some particles stuck in the fracture opening of 2500 μm compared to full removal with 3400 μm fracture. *Pill 1* and 5 experienced full removal of particles. The observed particles in some of the fractures, may indicate that reverse flow with brine resulted in a partial breakage of the filter cake, enabling the brine to flow through. The observations of particles in the fracture did not show consistent correlation with the results of the pressure needed to flow brine through the fracture. Hence, further testing should be done to investigate the consistency of the results, and whether CaCO₃ can regulate the ability to remove a pill from the fracture.

4. Sources of error / Lessons learned

Experimental set up:

- For the experimental method to remove the filter cake from a fracture, occasionally some particles were observed between the inside of the fluid cell and the disc housing. Hence the values for pressure needed to remove the filter cake may not be correct.

Measurements:

- For the fluid loss tests with Sample 9-11, the weight setting on the Ohaus logging weight was wrong and did not register small mass changes, hence the fluid loss curve only shows values up to 3.5 minutes.
- Only a small sample of the filtrate was applied for tests conducted for filtrate analysis, thus the value of polymers may not be correct.

5. Conclusion

The key findings of this thesis are:

- Use of grinding rod resulted in almost total degradation of CaCO₃ particles larger than 53 μm, while fiber particles did not show sign of particle degradation.
- Fluid loss test support that the sealing ability depends on PSD and that it deteriorates with degradation of CaCO₃ particles.
- With the modified starch as filtrate control, fluids with only CaCO₃ and fluids with a combination of CaCO₃ and fibers all gave a high degree of retained permeability, and hence present interesting alternatives for non-damaging reservoir drilling fluids.
- Inclusion of fiber consistently gave lower fluid loss and reduced polymer volume and concentration in the filtrate.
- The filtrate analysis on disc tests resulted in slightly higher variation in polymer concentration than tests on filter paper.
- The crosslinked potato starch was ineffective in preventing fluid loss and formation damage and showed a reduced ability to maintain viscosity after hot-rolling compared to modified starch.
- All LCM pills sealed the fracture up to the test limit of 4500 psi (31 MPa).
- Addition of CaCO₃ to the LCM squeeze pills significantly reduced the thickness of the filter cakes.
- While all the LCM pills successfully sealed the fracture up to 4500 psi (31 MPa), the pressure needed for full or partial breakage of the filter cake was consistently lower when CaCO₃ was added.

6. References

- Alsaba, M., Nygaard, R., Saasen, A., & Nes, O. M. (2014). Lost Circulation Materials Capability of Sealing Wide Fractures. *SPE-170285-MS*. <https://doi.org/10.2118/170285-MS>
- Green, J., Patey, I., Wright, L., Carassa, L., & Saasen, A. (2017). The Nature of Drilling Fluid Invasion, Clean-Up, and Retention During Reservoir Formation Drilling and Completion. *SPE-185889-MS*, 14.
- Khalifeh, M., Klungtvedt, K. R., & Vasshus, J. K. (2019). Drilling Fluid - Lost Circulation Material. *SPE-195609-MS*, 14.
- Khan, R., Kuru, E., Tremblay, B., & Saasen, A. (2007). Extensional Viscosity of Polymer Based Fluids as a Possible Cause of Internal Cake Formation. *Energy Sources*, 29, 1521-1529.
- Klungtvedt, K. R., Khalifeh, M., Saasen, A., Berglind, B., & Vasshus, J. K. (2021). Preventing Drilling Fluid Induced Reservoir Formation Damage. *SPE/IADC-202187-MS*, 24.
- Klungtvedt, K. R., & Saasen, A. (2022a). Comparison of Lost Circulation Material Sealing Effectiveness in Water-Based and Oil-Based Drilling Fluids and Under The Conditions of Mechanical Shear and High Differential Pressure. *Journal of Energy Resources Technology*, 10. <https://doi.org/https://doi.org/10.1115/1.4054653> - Article in process of being published.
- Klungtvedt, K. R., & Saasen, A. (2022b). Invasion of CaCO₃ Particles in Porous Formations in Presence of fibres. *Journal of Petroleum Science and Engineering*, 215. <https://doi.org/https://doi.org/10.1016/j.petrol.2022.110614>
- Klungtvedt, K. R., & Saasen, A. (2022c). A Method for Assessing Drilling Induced Formation Damage in Permeable Formations using Ceramic Discs. *Journal of Petroleum Science and Engineering*, 213. <https://doi.org/https://doi.org/10.1016/j.petrol.2022.110324>
- Klungtvedt, K. R., & Saasen, A. (2022d). The Role of Particle Size Distribution For Fluid Loss Materials On Formation Or Filter-Cakes And Avoiding Formation Damage. - Article in process of being published.
- Klungtvedt, K. R., Saasen, A., Vasshus, J. K., Trodal, V. B., Mandag, S. K., Berglind, B., & Khalifeh, M. (2021). The Fundamental Principles and Standard Evaluation for FLuid Loss and Possible Extencions of Test Methodology to Assess Consequences for Formation Damage. *Energies*, 14, Article 2252. <https://doi.org/10.3390/en14082252>
- Skjeggstad, O. (1989). *Boreslamteknologi, teori og praksis*. Alma Mater Forlag AS.

Appendix A

Procedure for measuring change in disc mass and change in permeability and relevant calculations following Klungtvedt, Saasen, et al. (2021).

1. Mix drilling fluid according to the recipe;
2. Measure pH and rheology;
3. Hot-roll and if applicable degrade by high-shear stirring or other degradation method;
4. Measure pH and rheology after hot-rolling and any degradation;
5. Mark and weigh disc in dry condition using the moisture analyzer (M_b). Moisture analyzer shall be set to dry disc at 105 °C until change in mass is less than 1 mg/60 s;
6. Optional step: place disc in acrylic cell and measure air temperature and flowrate at different pressures to calculate average permeability to air (K_{ab});
7. Optional step: place disc in acrylic cell and place arrangement with water in vacuum (circa -0.96 bar for 5 min) to remove any air from disc or water. Flow thereafter water through disc and measure water temperature and flowrate at different pressures to calculate average permeability to water (K_{wb});
8. Soak disc in brine (40 g NaCl per 1000 g freshwater) in vacuum;
9. Conduct HTHP test at desired pressure, typically 3.45 MPa (500 psi) or 6.9 MPa (1000 psi), and measure both volume (V_f) and mass (M_f) of fluid filtrate at point in time of 15 s, 30 s, 1 min, 2 min, 3 min, 5 min, 10 min, 15 min, 20 min and 30 min (V_f). Calculate fluid filtrate density;
10. Weigh disc with filter-cake and observe filter-cake;
11. Place disc in acrylic cell and reverse flow with 1 L (40 g NaCl per 1000 g water) heated to 60 °C and then with 1 L water heated to 60 °C. Note pressure required to enable reverse flow through disc;
12. Optional step: place disc in breaker fluid for required time and at required temperature. Place disc in acrylic cell and flow disc with 1 L water at ambient temperature to remove any dissolved filter-cake residue;
13. Optional step: place disc in acrylic cell and place arrangement with water in vacuum to remove any air from disc or water. Flow thereafter water through disc and measure water temperature and flowrate at different pressures to calculate average permeability to water (K_{wa});

14. Weigh disc in dry condition using moisture analyzer (M_a) using the same settings as in step 5;
15. Optional step: place disc in acrylic cell and measure air temperature and flowrate at different pressures to calculate average permeability to air (K_{aa}).

Depending on the number of optional steps included in the procedure, it enables collection of a large amount of data in addition to observing the filter-cake and the fluid filtrate volume V_f .

The moisture analyzer used for weighing the discs was set to heating the discs to 105 °C and continue drying until the mass change due to moisture evaporation was less than 1 mg per 60 s. The drying process then stopped automatically, and the mass of the disc displayed. The precision of the instrument is 1 mg. The change in disc mass was then simply calculated as:

$$(M_a) - (M_b) = M_{\text{change}}$$

By placing a digital weight under the graduated cylinder used to measure fluid filtrate, it was possible to simultaneously record the mass of the fluid filtrate and read the volume of the filtrate. This enabled a precise estimation of the fluid loss profile and calculating the fluid filtrate density (D_f), calculated as:

$$(M_f)/(V_f) = (D_f)$$

The permeability was calculated as an average of multiple readings within certain flow-rate ranges. Darcy's law was used in a rearranged form as follows:

$$K = \eta \frac{Q * \Delta L}{A * \Delta P}$$

where K is the calculated permeability coefficient (m^2), η is the viscosity of the fluid ($Pa * s$), Q the fluid flowrate (m^3/s), ΔL the disc thickness (m), A the areal of flow into the disc and ΔP the pressure differential over the disc (Pa).

Appendix B

Table B-1: Recipe and mixing sequence for samples 1-8 in grams unless stated otherwise

	Fluid 1	Fluid 2	Fluid 3	Fluid 4	Fluid 5	Fluid 6	Fluid 7
Sample size (mL)	350	350	350	350	350	350	350
Water	318.5	317.9	318.2	317.0	318.2	316.9	316.9
Soda ash	0.02	0.02	0.02	0.02	0.02	0.02	0.02
Caustic Soda	0.25	0.25	0.25	0.25	0.25	0.25	0.25
XC	1.3	1.2	1.5	1.4	1.6	1.5	1.5
Starch	6.0	6.0	6.0	6.0	6.0	6.0	6.0
Polymer	1.0	1.0	1.0	1.0	1.0	1.0	1.0
MgO	1.0	1.0	1.0	1.0	1.0	1.0	1.0
NaCl	20.0	20.0	20.0	20.0	20.0	20.0	20.0
CaCO ₃ (9 µm)					10	10	
CaCO ₃ (<23 µm)	10.0	10.0	10.0	10.0	10.0	10.0	10.0
CaCO ₃ (<53 µm)	10.0	10.0	10.0	10.0	10.0	10.0	10.0
CaCO ₃ (50 µm)	20.0		20.0		10.0		10.0

Table B-2: Recipe and mixing sequence for fluid with crosslinked potato starch (Samples 9-11) in grams unless stated otherwise.

	Base 8	Base 9
Sample size (mL)	350	350
CaCl ₂ Concentration	34.28	34.28
Water Concentration (mL)	313.6	313.6
Bactericide	1.3	1.3
MgO	1.0	1.0
Corrosion Inhibitor	1.45	1.45
Defoamer	1.25	1.25
Oxygen Scavenger	0.35	0.35
Lubricant	5.2	5.2
CaCO ₃ (10 µm)	9.99	9.99
CaCO ₃ (25 µm)	9.99	9.99
CaCO ₃ (50 µm)	9.99	9.99
Crosslinked Potato Starch	7.99	7.99
Hydrogen Sulphide Scavenger	1.36	1.36
Alkalinity Control	1.7	1.7
Viscosifier (XC polymer)	1.5	1.3

Table B-3: Name and amount additives used in the mixtures.

	Name	Amount (g)
Additive 1	FEBRICOAT C	8.0
Additive 2	AURACOAT UF	5.0
Additive 3	AURACOAT F	5.0
Additive 4	AURAFIX UF	5.0

Table B-4: Recipe for LCM Pills (Samples 12-16) in grams unless stated otherwise.

	Pill 1: 122.5 lbs/bbl CaCO ₃	Pill 2: 90 lbs/bbl CaCO ₃	Pill 3: no CaCO ₃	Pill 4: 40 lbs/bbl CaCO ₃	Pill 5: no CaCO ₃
Sample size (mL)	350	350	350	350	350
Water	280.1	244.9		285.0	299.8
5 % NaCl water			290.5		
XC	1.4	0.5	1.0	0.5	0.5
Starch	6.0				
Polymer	1.0				
MgO	1.0				
NaCl (sea salt)	41.0	41.0		41.0	41.0
Additive 6		60.0	60.2		
Additive 5				30.0	30.0
Additive 1				10.0	10.0
CaCO ₃ (<53 μm)		75.0		40.0	
CaCO ₃ (50 μm)	17.5	15.0			
CaCO ₃ (150 μm)	35.0				
CaCO ₃ (600 μm)	35.0				
CaCO ₃ (1200 μm)	35.0				

Appendix C

Figure C-1: Tapered discs after pressure tests for pills with inclusion of CaCO_3

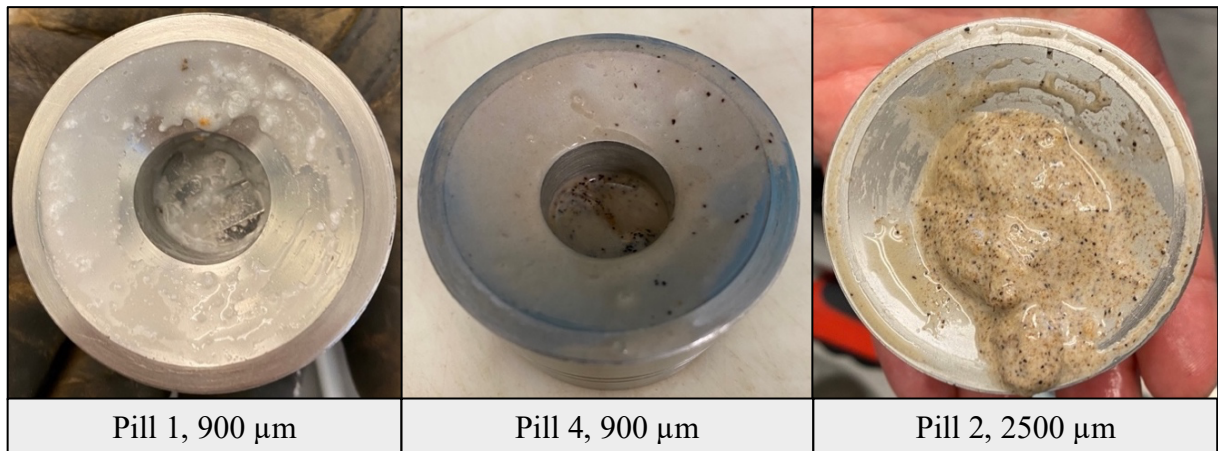


Figure C-2: Tapered discs after pressure tests for pills with no CaCO_3



Appendix D

Figure D-1: Discs with filter cakes for fluids with crosslinked potato starch and fluids with modified starch after fluid loss tests.



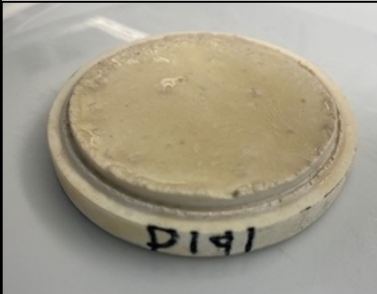




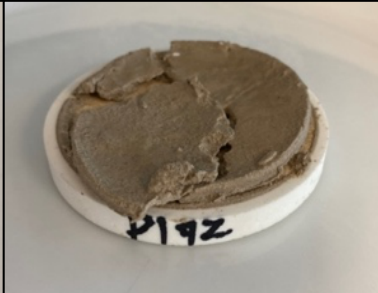

Modified Starch			
	Base with 9 μm CaCO_3	Base with 9 μm CaCO_3 + Additive 2	
CPS			
	CPS Base	CPS Base + Additive 2 (XC 1,5)	CPS Base + Additive 2 (XC 1,3)

Figure D-2: Discs used for testing fluids with crosslinked potato starch and fluids with modified starch, after filter cake removal with reverse flow.

Modified Starch			
	N/A	Base with 8 μm CaCO_3 + Additive 2	
CPS			
	CPS Base	CPS Base + Additive 2 (XC 1,5)	CPS Base + Additive 2 (XC 1,3)